

POLITECNICO DI TORINO & UTC DE COMPIEGNE

DEPARTMENT OF MECHANICAL AND AEROSPACE ENGINEERING

Master of science in Mechanical Engineering

Master's thesis

Design of a linear actuated Electrohydraulic servo valve for
tree shaker applications with the hydraulic test bench .



Supervisor UTC Compiègne:

Prof. Eric Noppe

Department of Fluid power Compiègne, France

Student:

Dzomene Feupi Armand Joel

S242595

Supervisor Politecnico di Torino

Prof.ssa Daniela Anna Misul

Department of Energy Torino, Italy

April 2021



Acknowledgements:

At the end of this work, I would like to express my deep gratitude to my UTC's supervisor Mr. Eric Noppe for his follow-up and for his enormous support throughout the whole project period.

I thank Mr. Olivier Tourneur for his internship visit and his lively interaction between Pack'Aéro and the hydraulic platform.

I would also like to thank my UTC Tutor Mr. Benoit Souyris for his follow-up and his internship visit.

I thank my Polito Supervisor Prof. Daniela Misul for the advises and the support.

My thanks go to all the staff and fellow interns of the UTC's Fluid power-Mechatronics Laboratory for their great assistance.

Finally, my thanks to all those who contributed directly or indirectly to the smooth running of this project.



1. CONTENTS

1. CONTENTS.....	2
2. GROUP WORK PRESENTATION.....	4
2.1. Presentation of the Fluid power platform	4
2.2. Presentation of the company Pack'aero	5
3. PRESENTATION, GOALS OF THE PROJECT AND DEFINITIONS.....	7
3.1 Presentation and goals	7
3.2 Descriptions and definitions	7
3.2.1 Servo valve Moog 62 (existing valve)	8
3.2.2 Electrohydraulic servo valve with linear actuator: « voice-coil ».....	11
3.2.3 Hydraulic test bench.....	13
4. PROJECT STEPS.	16
4.1 Experimental study: design of the hydraulic test bench.....	16
4.1.1 Description of the test measurements to be carried out on the valve	17
4.1.2 Manifold design and choice of the hydraulic components of the test bench..	19
4.1.2 Verification of deferent configuration of the test bench and final validation .	21
4.1.4. Results	26
4.2. Numerical validation	30
4.2.1 Computational fluid dynamic (CFD) with Ansysfluent.....	31
4.2.1.1 Description of geometry and volume extraction for the CFD simulation	32
4.2.1.2 Valve Assembly and volume extraction	33
.....	34
4.2.1.3 Preparation and simplification of the fluid volume for the CFD	34
4.2.1.4. 3D model in quasi-stationary approach	35
4.2.1.5 Meshing	35
4.2.1.6. Study of the sensitivity to the number of meshes for a 0.9 mm.....	37
4.2.1.7 Boundary conditions and properties of the fluid	38



4.2.1.8.	Numerical schemes	39
4.2.1.9.	K-Epsilon model for turbulence.....	39
4.2.1.10.	Results of the CFD simulation	40
4.2.2.	Numerical modelling of the linear actuated servo valve and estimation of the force and size of the springs and the actuator with Amesim	46
4.2.2.1	Model of the hydraulic part without the linear actuator.....	47
4.2.2.2.	First estimation of the spring force for a maximum spool stroke (0.9mm). 48	
4.2.2.3	Design of the valve integrating the actuator and regulating the PID.....	50
4.3	Conclusion and Proposition of an improvement of the servo valve.....	55
5.	WHAT I LEARNED DURING THE STAGE.....	58
5.1.	Professional competencies acquired.....	58
5.2.	Software used.....	59
6.	CONCLUSION.....	60
7.	GLOSSAIRE.....	60
8.	Sources.....	61
9.	ANNEXES.....	62
9.1	Liste des Figures	62
9.2	Liste des tableaux.....	64
9.3	Nomenclature	65

2. GROUP WORK PRESENTATION

My project took place within the Hydraulic Platform of the Roberval Laboratory of UTC. This project was carried out on request of “**Pack'Aéro Mécatronique**” which is a French company producing mechanical and mechatronic components for aeronautic field and other industrial applications.

The project involves the development of a hydraulic servo valve solution with its test bench.

2.1. Presentation of the Fluid power platform



Figure 1: global view of the platform

This platform was built for R&D in 2014 on the initiative of the UTC, the **CETIM** (Centre Technique des Industries Mécaniques) and **ARTEMA** (Syndicat des industriels de la mécatronique).

The workshops of the Hydraulic platform are based on the ground floor of the UTC Innovation Centre. The platform contains 3 test benches, each of which has a link with the current expectations of the companies.

- The test bench for "Vibration and pulsation analysis": allows studies to be carried out to try to reduce the noise generated by hydrostatic transmissions.

- Test bench for "Energy and Modelling", it is used to carry out tests to control hydrostatic transmissions, in order to optimize them.

Regarding my project, I had to design a new test bench to carry out the various tests (pressure drop and flow measurements) on the servo valve designed. At the end of my internship, only the control part of the bench was completed and mounted, the hydraulic part was not mounted due to the order delay in ordering the drilled block to connect different elements of the test bench. However, the whole system was completely designed.

2.2. Presentation of the company Pack'aero



Figure 2 : PACK'AERO sites location



High precision mechanics, the origin of the group's reputation, is the historic heart of Pack'Aéro's activity. This is where one of the fundamental skills of the group resides, transmitted by several highly qualified generations.

Today, Pack'Aéro is a company that combines skills in mechatronics, electrical engineering and advanced electronics. For the company, mechatronics represents the technological challenge of tomorrow, in particular by the emergence of the concept of "more electric" in aeronautics and of "intelligent" systems for more performance, energy efficiency, safety and reliability. This also allows the group to offer clients products developed or co-developed for them.

Their key skills are also: Engineering (design / simulation / laboratory), rapid prototyping, development, qualification, industrialization, manufacturing, marketing and support; based on strong technological expertise in linear or rotary electromagnetic actuators with limited travel.

They offer many services in the aeronautical field such as the design of voice-coil actuator servo valves which is the subject of my internship.

The Pack'Aéro Group capitalizes over 50 years of experience built around high precision mechanics, with around 200 employees at 3 sites in France and Tunisia.

They provide services in a variety of fields (engineering / mechatronics, high-precision mechanics, production / assembly of parts of intermediate technicality), Pack'Aéro employees design, produce or process critical sub-assemblies for major contractors in high-tech industries.

The main customers are Safran Snecma, Turboméca, Sagem, Messier-Bugatti-Dowty, Hispano-Suiza, Airbus Helicopters, Dassault Equipements, Sames, Carmat and many others.

3. PRESENTATION, GOALS OF THE PROJECT AND DEFINITIONS

3.1 Presentation and goals

This study is based on the design of an electrohydraulic servo valve with a linear actuator (voice-coil) and its hydraulic test bench (including the control panel part for the data acquisition). The company's need is to design a linear actuated servo valve from an existing servo valve with motor-torque actuator. The advantage of this new solution is the leakage reduction in the valve, reduction of energy consumption at the equilibrium position of the slide, reduction of the response time by eliminating the hydraulic pilot control stage. This valve will find an application in vibrators agricultural machine for fruit harvest. This research and development work was carried out on the hydraulic platform of **UTC** of **Compiègne** in collaboration with **Pack'Aéro** company.

The work was articulated in several stages.

- Design of the hydraulic bench for the performance characterization of the existing servo valve, Moog62.
- Design and mounting of the electrical and electronic control panel box for the data acquisition on the test bench.
- CFD study of the servo valve to estimate the detailed pressure drops across the valve, the jet angle and the speed field using Ansysfluent software.
- Modelling of the servo valve with voice-coil linear actuator on Amesim, evaluation of the size of the springs and the characteristics of the actuator required.
- Simulation and comparison of the pressure and flow rate results from Ansys and Amesim .

3.2 Descriptions and definitions

An electrohydraulic servo valve is a hydraulic valve equipped with an automatic control device (actuator) allowing the control of its opening.

It transmits mechanical energy of translation or rotation (torque and speed of rotation) into mechanical energy of rotation through fluid power (flow and pressure difference between the inlet and outlet of the machines).

It has applications in many engineering fields such as production, aerospace, and agriculture. In general, it allows to control the motion of an hydraulic cylinder or motor allowing the latter to transmit a linear or rotary movement. They are used for example to control airplane's wings or even better as in our case to control the mechanical arm motion of an agricultural machinery such as a vibrator for fruit trees (fig 3).



Figure 3: Hydraulic tree shaker machine

3.2.1 Servo valve Moog 62 (existing valve)

-Description

This servo valve with a torque motor actuator is useful to design our new valve solution with a linear actuator.

The Moog 62 servo valve has 2 stages. The power stage is a classic proportional distributor with a spool, with zero overlap. (hence the need for great precision of realization which induces high costs). The objective of the control stage is to control the movement of the slide by creating a pressure difference ΔP between its 2 ends. This ΔP is obtained by a system of flapper-nozzles.

The position of the pallet located between the 2 nozzles is controlled by a torque motor. This flapper is extended by an elastic element called a cantilever spring. The end of this spring is housed in a groove in the spool.

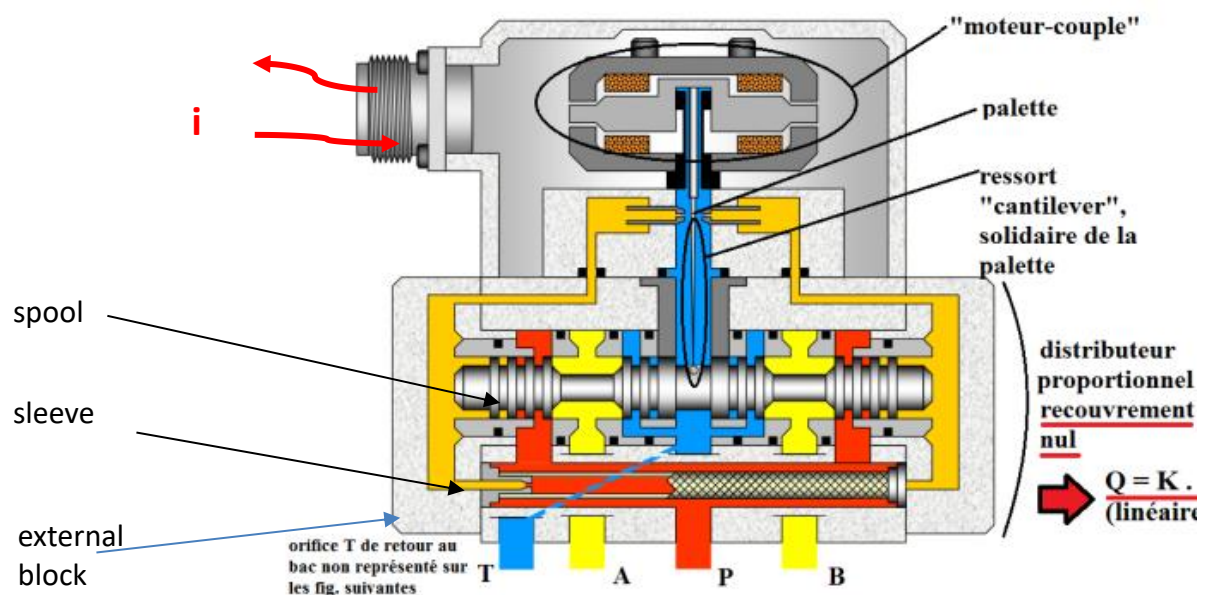


Figure 4: Working principle of the Moog 62 servo valve

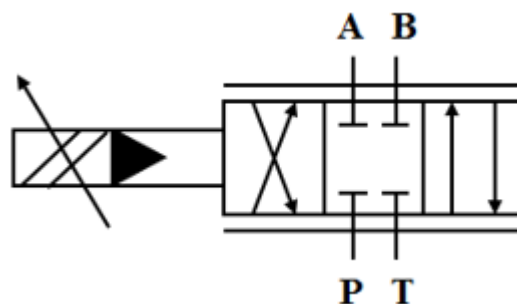


Figure 5: Schematic representation of the servo valve

➤ Working principle

There is no control current (i) (fig5-a), the flapper is in the central position between the 2 nozzles. The fluid coming from the port P passes through the orifices. The pressures of the fluid which feeds the 2 nozzles is identical. This pressure applies on the 2 sides of the spool and therefore remains in the central position. Ports A and B are therefore closed.

When the torque motor is controlled by a current signal i , the flapper moves toward one of the 2 nozzles (in this case, toward the one on the right) and therefore interferes with the outlet of the fluid through this nozzle. We therefore create an additional pressure drop that pressurize on the right side of the spool.

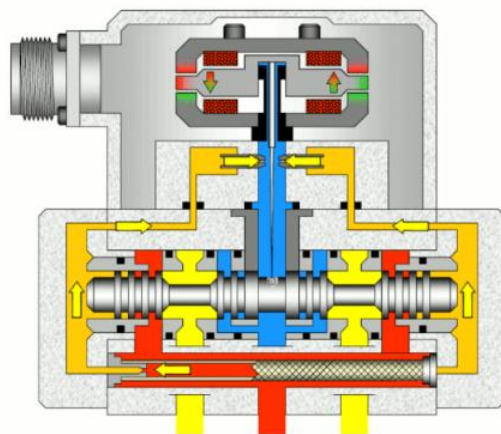


Figure 6-a Spool central position

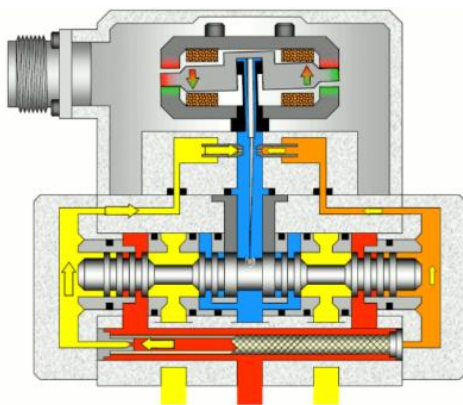
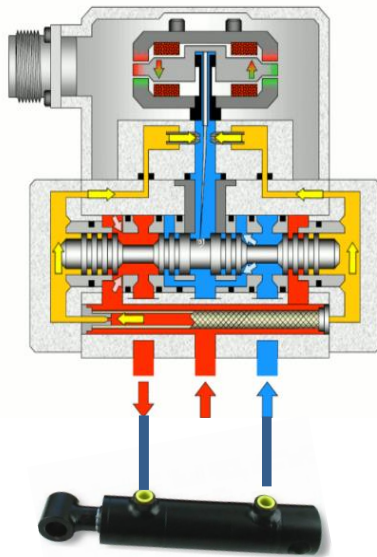


Figure 6-b : Spool left position

The spool moving to the left carries with it the end of the cantilever spring. This creates a torque that opposes that produced by the torque motor.

when the two torques are equal, the flapper has returned to the central position.



The pressures at the 2 ends of the spool are therefore again identical. The position of the slide is then stable and defined by the equality between the motor torque and the feedback torque of the cantilever spring. The position of the slide is then the image of the control current I .

There is therefore communication of the ports P and A with a flow rate Q proportional to the input current i .

Figure 6-C : Spool right position

3.2.2 Electrohydraulic servo valve with linear actuator: « voice-coil ».

Note: The only difference with the previous one (torque motor actuator) is the actuation mode which in this case is linear and the reduction in the number of stages. In fact for the voice-coil (figure 7) the pilot stage is removed this having advantages compared to the previous Moog 62 valve with motor-torque actuation. The advantages of this new solution are:

- Direct actuation therefore reduction of the time response
- Reduction of the number of stages by elimination of the pilot stage
- Reduction of leakages in the servo valve
- Reduced consumption at rest because unlike the Moog 62 which uses pressurized fluid to keep the spool at the central position, the voice-coil does so thanks to the two springs at the ends of the spool (fig-7)

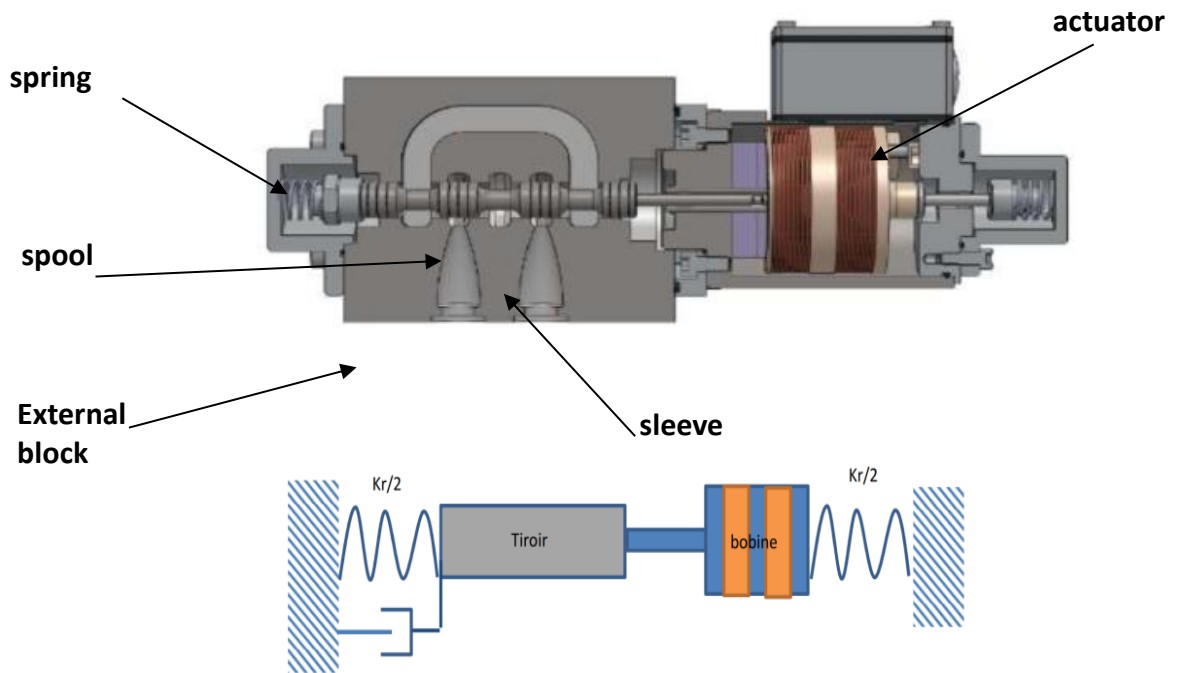


Figure 7: servo valve with linear actuator

➤ Working principle of the linear actuator, voice coil.

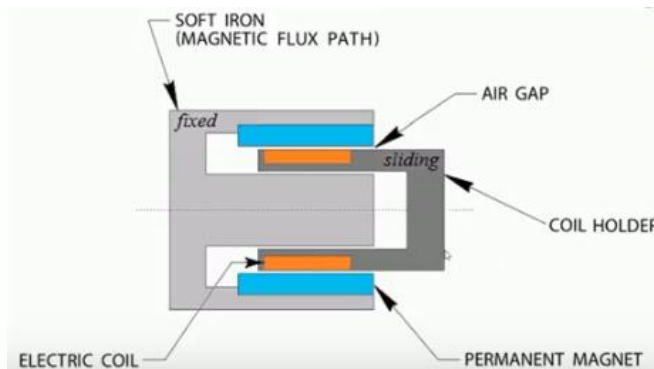


Figure 8: linear actuator voice coil

The working principle is identical to that of a conventional loudspeaker. In fact to generate a displacement therefore a force of the actuator on the slide of the servovalve by using the magnetic field to generate a force of lorenz.

Fig-8 bellow shows the orientation of the actuator force when the direction of the current is reversed.

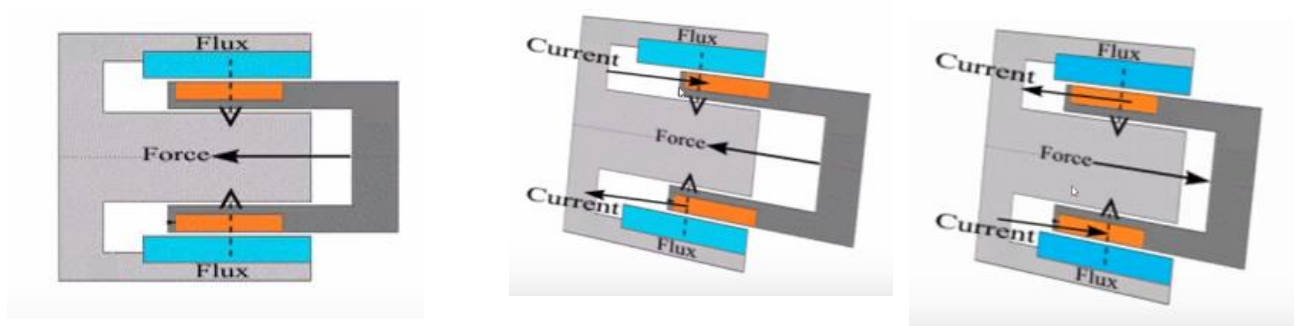


Figure 8: Force orientation according to the magnetic field

3.2.3 Hydraulic test bench.

The test bench is used to realise tests on the servo valve to determine its static and dynamic performances.

Figure 9 below shows the interaction between the hydraulic test bench, the servo valve and the dynamic cylinder.

The system consists of a hydraulic unit with a powerful pump, a drilled block connects two accumulators, electro valve(to control the fluid direction) ,a servo valve ,a dynamic cylinder .the data acquisition and control system and several sensors complete the test bench and allow the validation of the model and the implementation of different control laws.

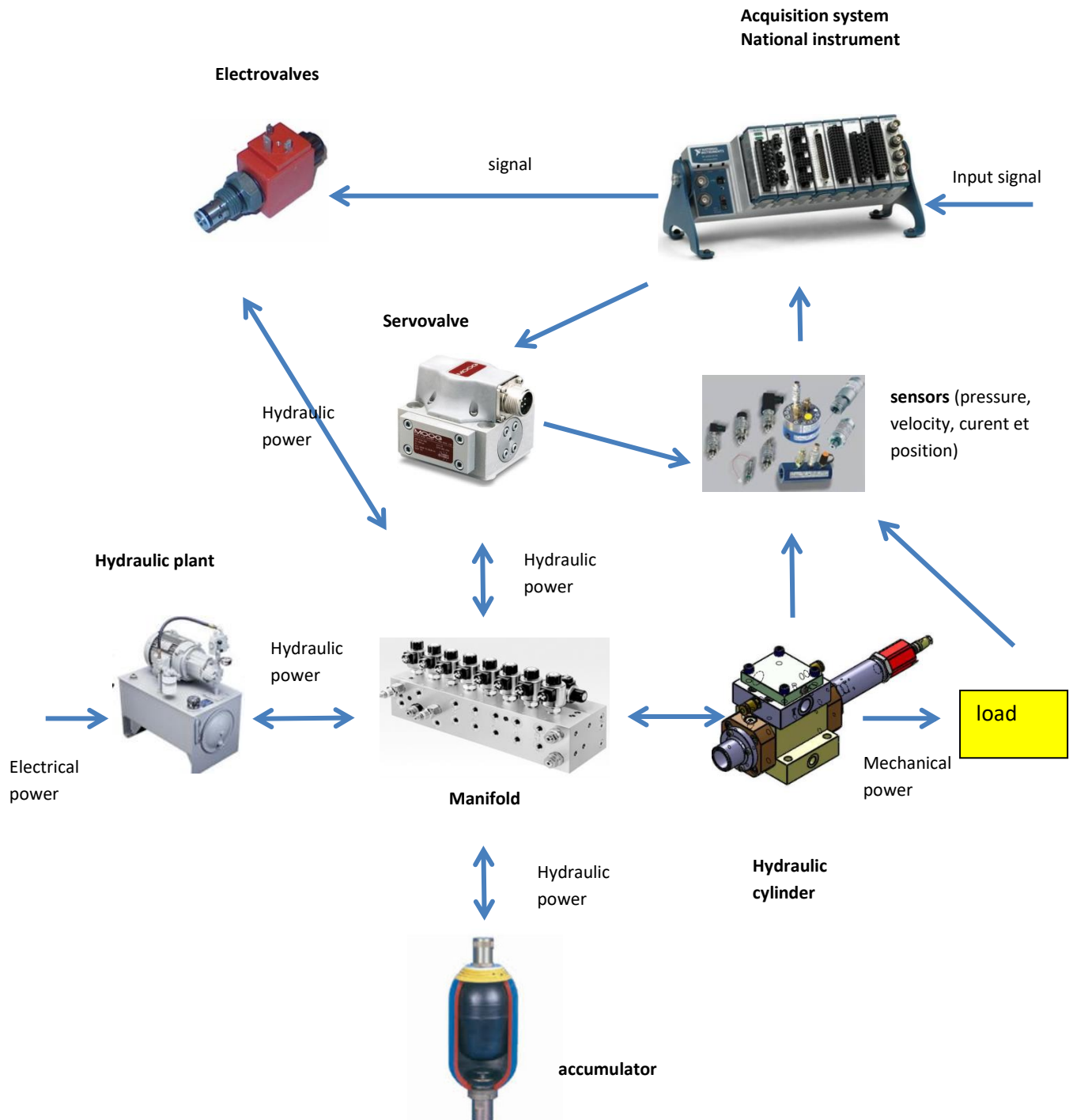


Figure 9: general overview system bench-servo valve

The hydraulic test bench is used to perform dynamic and static tests to characterize the performance of the servo valve.

This hydraulic test bench consists of the following elements, each with a well-defined function (fig. 7):

- **Hydraulic pump:** Converts mechanical energy (supplied by the motor thermal) into hydraulic energy.
- **Electric motor:** Used to drive the hydraulic pump.
- **Booster pump:** Used to supply oil to the hydraulic circuit for compensating external fluid leakages and intensify the pressure in the. This pump is integrated in the hydraulic pump.
- **Pressure limiter:** Protection devise to avoid an excessive increase in pressure in The circuit protecting the installation and its components.
- **Heat exchange:** Prevents excessive heating of the fluid in the transmission. It is also this same fluid that makes it possible to evacuate part of the heat produced by mechanical parts of hydraulic machines. This exchange is always performs on the low-pressure branch of the circuit.
- **Filtration:** Filters the fluid to avoid the circulation of impurities in the hydraulic circuit that could damage the transmission.
- **Electrohydraulic servo valves:** used for controlling powerful hydraulic machines with small electric signal (we will see the importance of this component later).
- **Reservoir:** Used to store the fluid circulating in the circuit.
- **Manifold:** Used to mount all the hydraulic components to have a more compact system.
- **Solenoid valves:** Used to set up different circuit paths for testing channels of the servo valve.
- **Pressure sensors:** Measure pressure variations across the servo valve.
- **Flowmeters:** Used to carry out flow measurements through the different servo valve channels.

- **Dynamic cylinder:** Used to study the dynamic performance of the servo valve by plotting the Boode diagram and the frequency response.
- **Accumulator:** Ensures a constant pressure in transient mode by providing the missing flow in the circuit in time due to a fast change in the displacement of the pump / motor, the main pump being unable to control the pressure in the circuit in time. This allows the pressure in the circuit to be adjusted quickly.

4. PROJECT STEPS.

4.1 Experimental study: design of the hydraulic test bench.

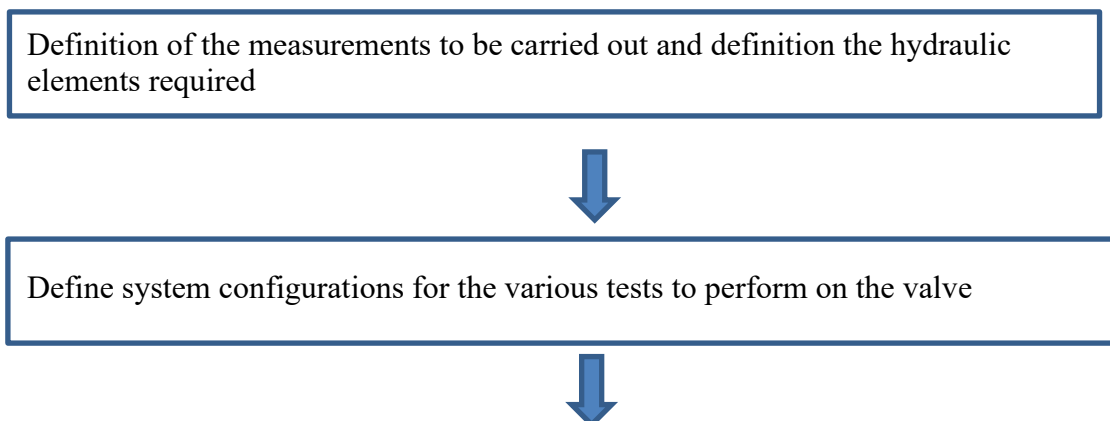
The test bench is made by two part:

- Hydraulic part power by the fluid
- Control part to control the test bench and acquires data measured

The hydraulic bench is used to carry out measurements on the existing Moog 62 hydraulic servo valve whose spool and sleeve will be used to design the linear voice-coil servo valve. "These measurements will be useful to check the reliability of the test bench. Once the latter has been designed, measurements will be made using the test bench.

➤ Design of the Hydraulics test bench part

The following steps show how the hydraulic part was designed:



Choice of solenoid valves, sensors, dynamic cylinder, accumulator, protective elements.



Definition of the drilled block(manifold) and check if it allows carrying out all measurements



Final validation and check of the block before manufacturing

4.1.1 Description of the test measurements to be carried out on the valve

A) Configurations for static test measurements to be performed

The figures below describe the various tests to be performed on the servo valve. The first three are used to determine the flow rates between different orifices of the valve. The fourth, on the other hand, to measure leaks and pressure drops in the valve.

1- Configuration to measure the flow between ports A and B

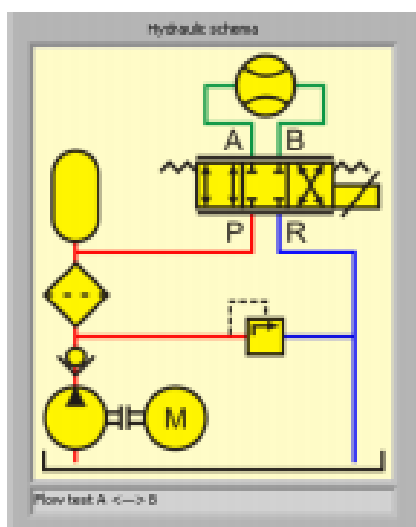


Figure 10-A: flow measurement from A to B

2- Configuration to measure the flow between ports A and T(R)

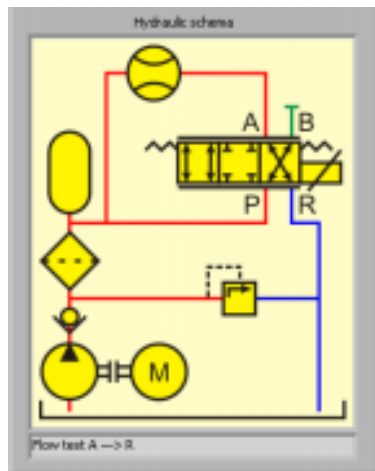


Figure 10-B: flow measurement from A to R

3- Configuration to measure the flow between ports B and T(R)

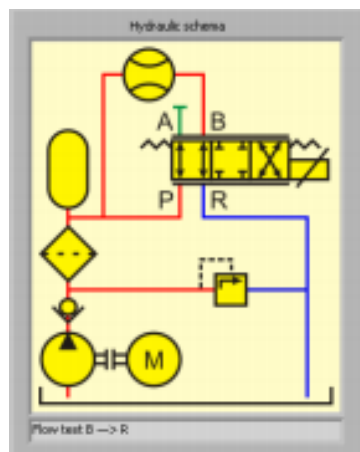


figure 10 C: flow measurement from B to R

4-Configuration for measuring leakages and pressure drops

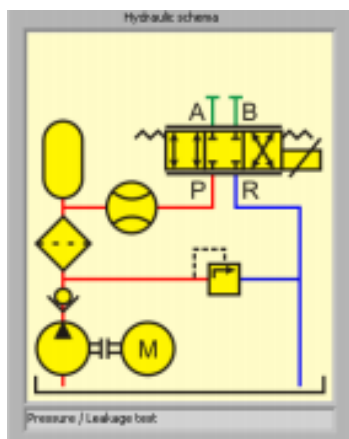


Figure 10-D: leakages and pressure drop

A) Configuration to measure the frequency and step response

Finally, for dynamic tests, the flow meter is replaced by a dynamic cylinder (fig-12) to no longer determine the flow and pressure drop but rather to determine the frequency and step response of the system.

These dynamic characteristics determine the stability of the valve and its ability to follow a current setpoint imposed on it for a certain movement of the slide.

➤ Configuration to measure the frequency and step response

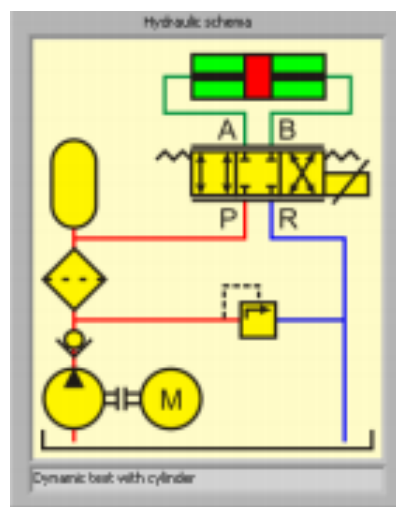


Figure 12 : configuration for dynamic tests

4.1.2 Manifold design and choice of the hydraulic components of the test bench

The analysis of different configurations of the tests to perform static and dynamic described above made it possible to obtain the configuration of the manifold as indicated in a **figure 13** below

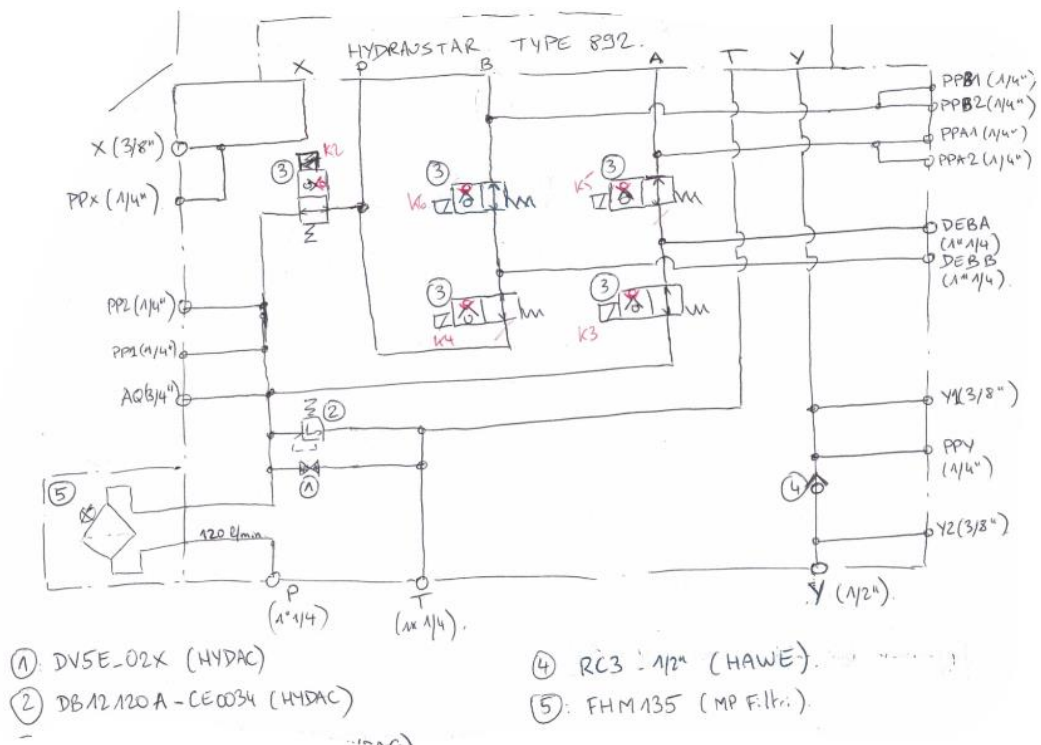


Figure 13 : Manifold

The limit conditions of use of the bench are very important in choosing the components. Indeed, these components must be chosen taking into account the maximum pressures and flow rates in the circuit. The specifications indicate the following maximum quantities:

$$Q_{\max}=110\text{l/min}$$

$$P_{\max}=220\text{bar}$$

The following components of the circuit were selected according to these two parameters and many others.

Table 1 below summarizes all the necessary components for the good functioning of the bench.

Hydraulic test bench components	Quantity
Accumulator Leduc 2,5L	1
Electro valves (GS06-86-0-0-N-SP/ss-DO24D) 90l/min-350bar-24 vdc Imax=800mA	5
flowmeter VS02 , alim 10-28VDC, Pmax=400bar	1
flowmeter VRZ , power supply 15/24DC, Pmax=400bar, Q=1-400l/min	1
Pressure sensor, 250bar max, 7 → 28 V, IP65, precision ±0,1 %	3
Flow restrictor -110l/min ,400bar	1
Flow restrictor 30lpm, 350bar	1
Filter 450lpm ,320bar	1
Servo valve moog 62, + /-50mA serie configuration (+ /-100mA parallele) Imax=100mA	1
Dynamic hydraulic cylinder ,6pin, alim 24vdc ,output speed +/-10 Vdc ,output displacement 0-10vdc	1
Non-return valve 60l/min, 500bar	1
Manifold	<u>1</u>

Tab 1: Hydraulic components list

4.1.2 Verification of deferent configuration of the test bench and final validation

The combination of the solenoid valves in the open or closed position makes it possible to carry out the various configurations for carrying out the tests mentioned above. Figures 14 make it possible to verify whether the system actually allows to perform the desired tests to be carried out. Three colours have been used to indicate the fluid pressure levels in the circuit:

- **Red:**

Red indicates high pressures up to 250 bar

- **Blue:**

Blue indicates low pressure, tank pressure.

- green:

Intermediate pressures.

Note: The tables below with the notations from K1 to K5 represent the solenoid valves states

1- Flow rate measurement from A to B.

électrovannes	Etat
K1	on
K2	On
K3	On
K4	Off
K5	off

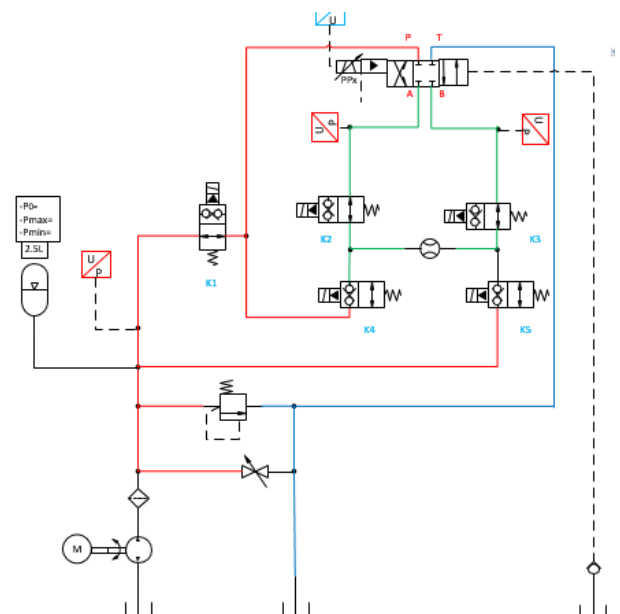


Figure 14-A: Flow rate from A to B

2- Flow rate measurement from A to T.

électrovannes	Etat
K1	Off
K2	On
K3	Off
K4	Off
K5	on

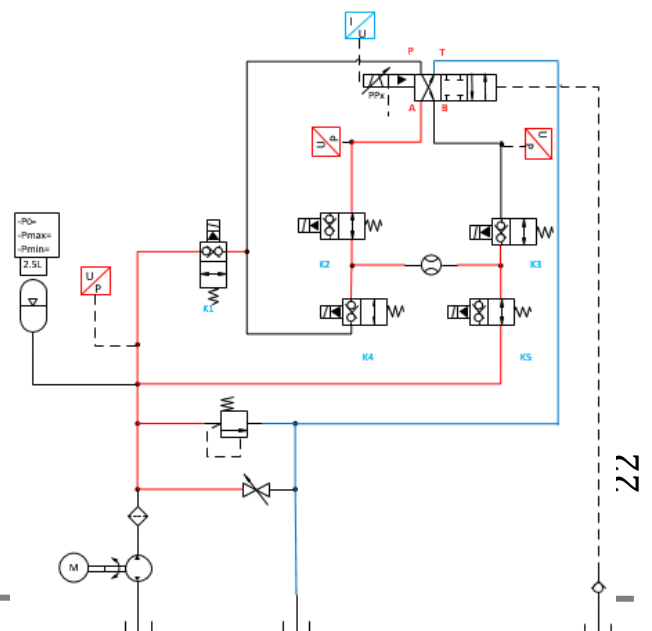


Figure 14-B: flow rate from A to T

3- Flow rate measurement from B to T.

électrovannes	Etat
K1	On
K2	Off
K3	On
K4	On
K5	off

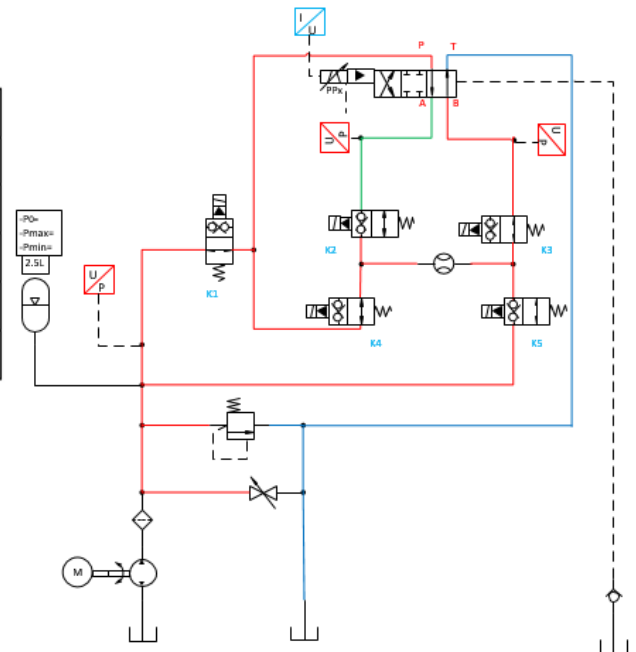


Figure 14-C: Flow rate from B to T

4- Leakages and pressure drop.

électrovannes	Etat
K1	off
K2	Off
K3	Off
K4	On
K5	on

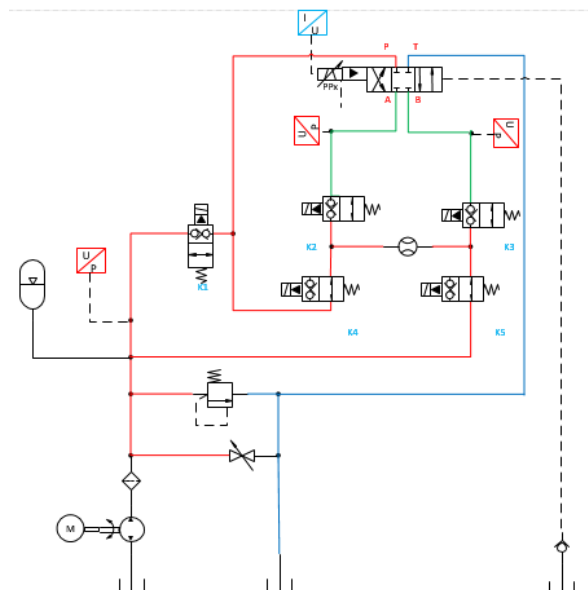
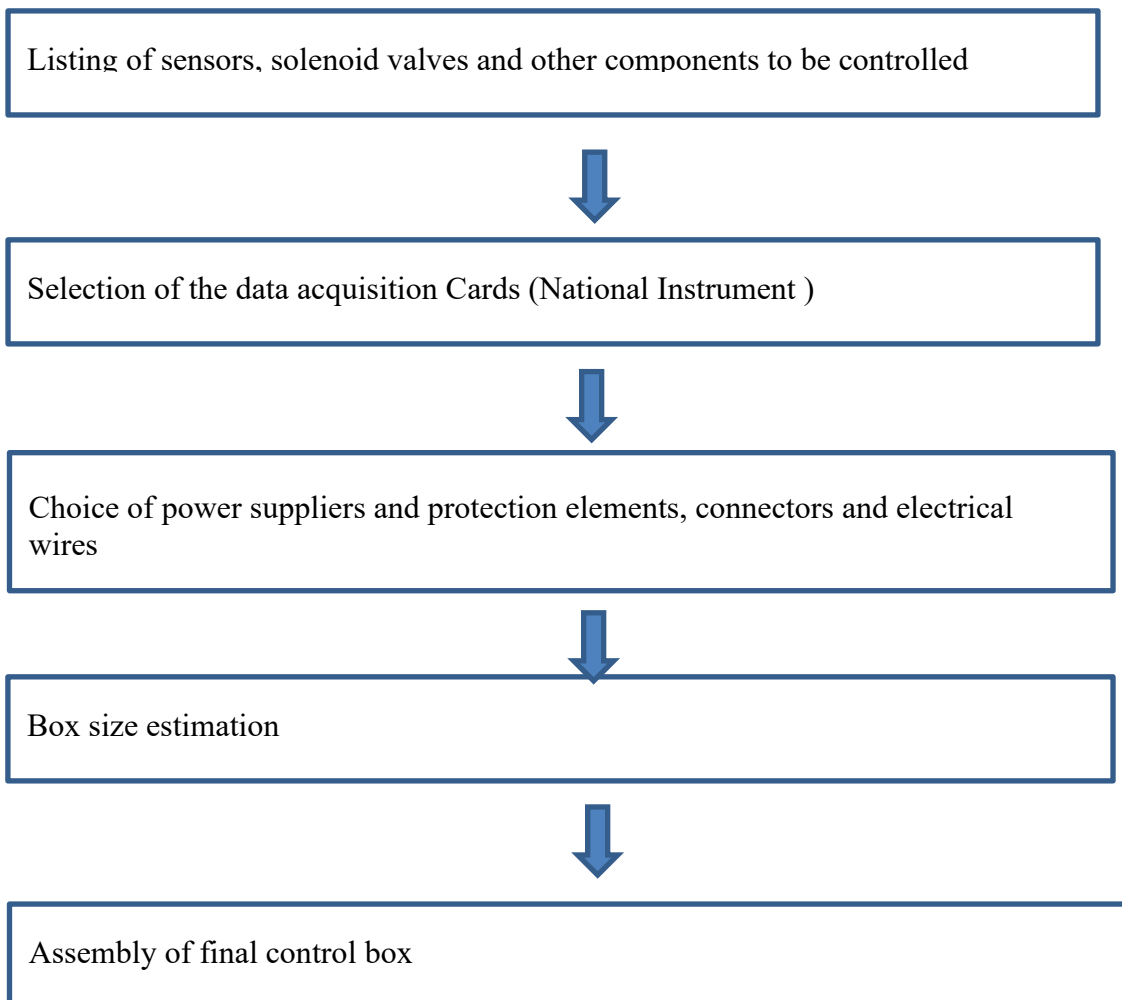


Figure 14-D: leakages and pressure drop

➤ **Design of the electrical and electronic control box and definition of the data acquisition system**

The control box constitutes the bench acquisition system. In fact, it supplies power to all bench components such as sensors, servo valve, solenoid valves, acquisition cards and amplifiers.

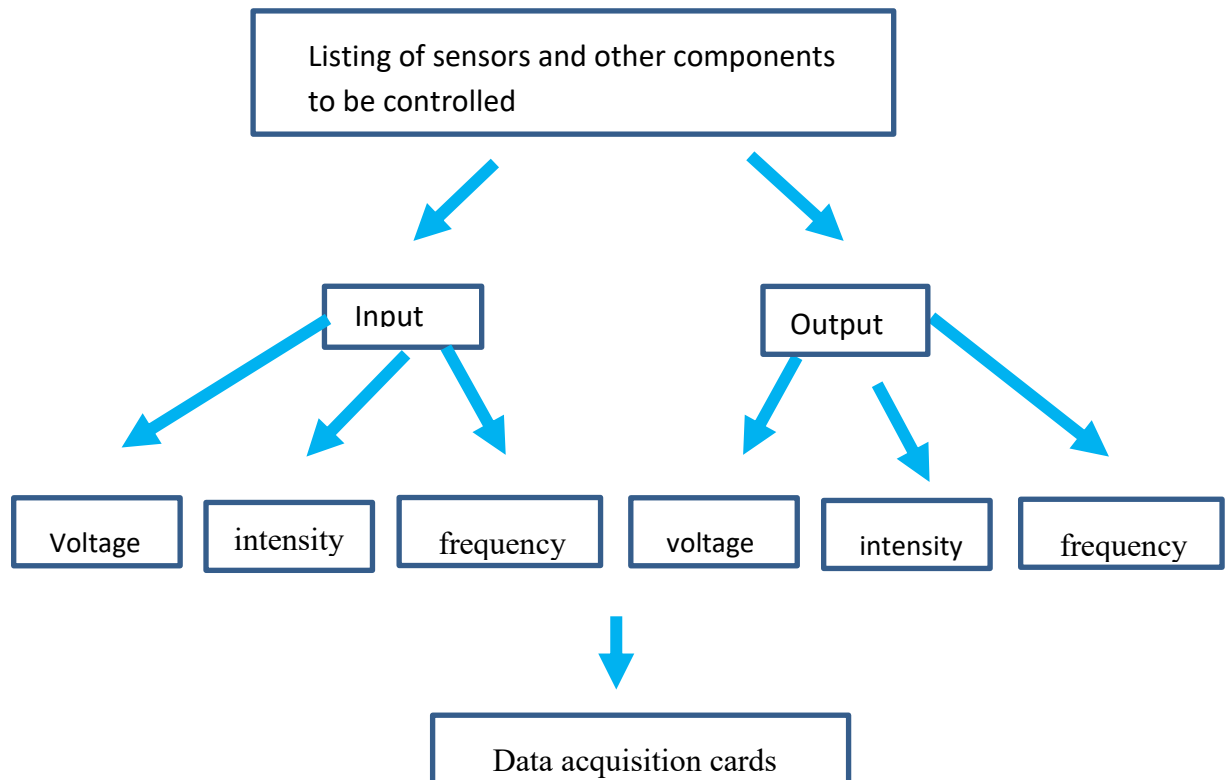
The steps for the design of the case are as follows:



➤ **Data acquisition material selection.**

To make a good choice of the data acquisition system equipment, it is better to start by listing all the sensors and classifying them into input and output. After that, in each input / output sub-group, group the sensors according to the type of signal (voltage / current / frequency) and finally select the acquisition cards.

The diagram below summarizes this procedure



	Modules	Code		Prix(€)
Ni-daq	Module pour vérin, sonde de la Voie call 16 entrées analogiques différentielles	NI-9205	1	895 €
	Module pour capteur pression	NI9203	1	590 €
	Module pour débitmètre VRZ	NI9361	1	695 €
	Module servo valve Moog62 et voice-coil ,4 sorties analogiques	NI 9263	1	455 €
	Module électrovalves, 8 entrées digitales	Ni 9472	1	106 €
	Châssis c-daq 9174	cDAQ-9178	1	1.420 €

Tab 2: data acquisition system components list

4.1.4. Results

➤ **Signal distribution (sensors +data acquisition cards).**

Fig 14 below shows the distribution of the sensors according to the type of signal and the direction (input / output) of the signal.

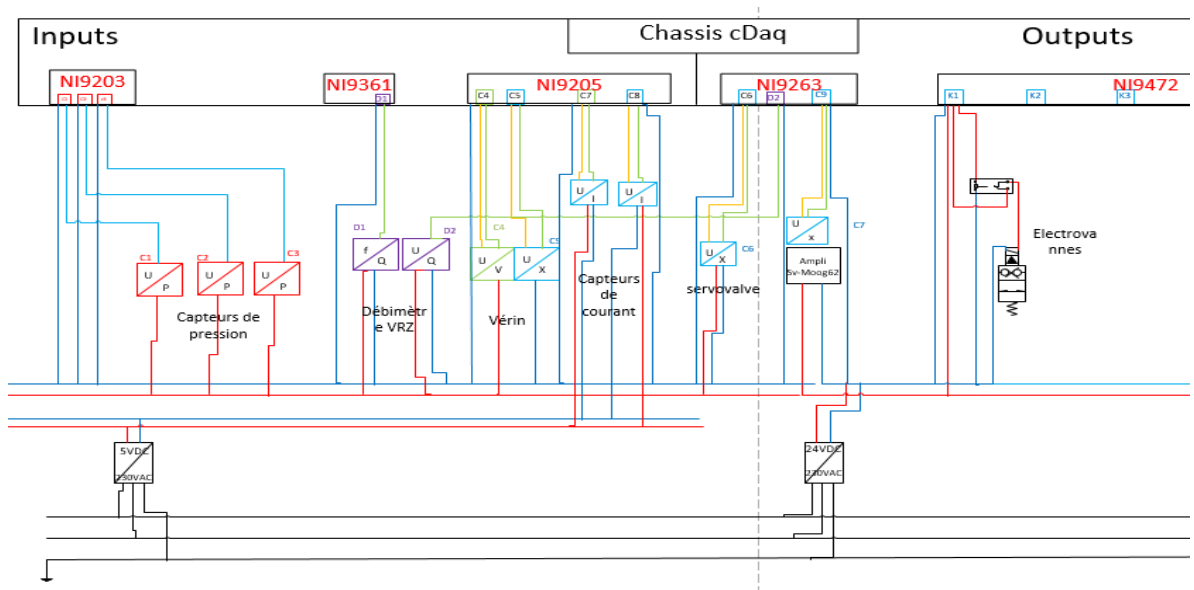


Fig 15: Signal distribution (sensors+cards)

➤ **Electrical scheme of the test bench's box**

Fig-16 below shows the electric and signal circuit of the bench control unit.

The elements have been divided into two stages. The upper stage contains the electrical components and the lower one contains the electronic components for acquisition. This separation helps prevent electrical currents from interfering with the signal data.

Légende:

- Phase
- Neutre } 230AC
- Terre
- Phase
- Neutre } 24/5 DC
- Signal

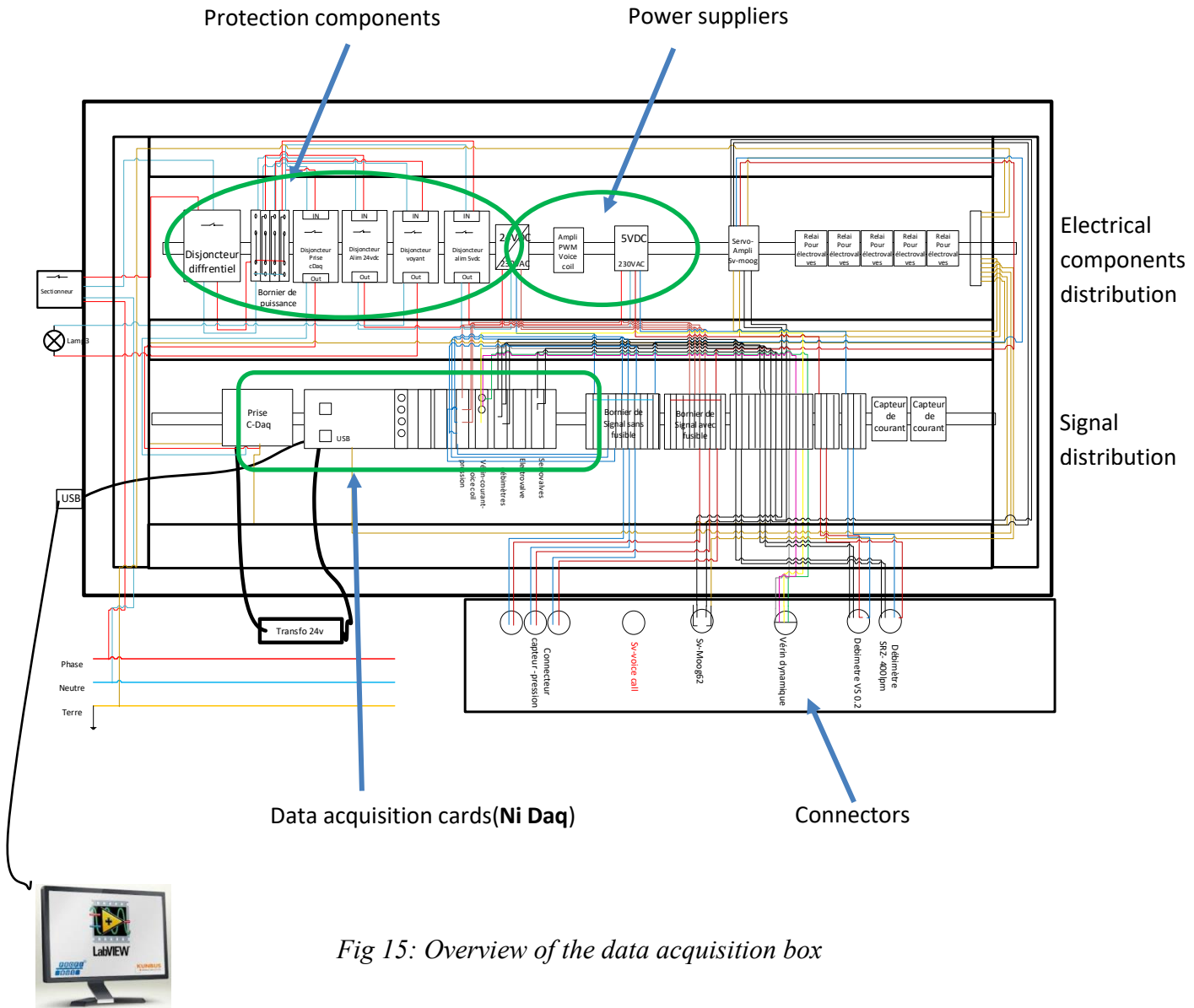


Fig 15: Overview of the data acquisition box



Fig 16: Box drilling holes process



Fig 17 : rails fixation, components mounting on the supports and cabling

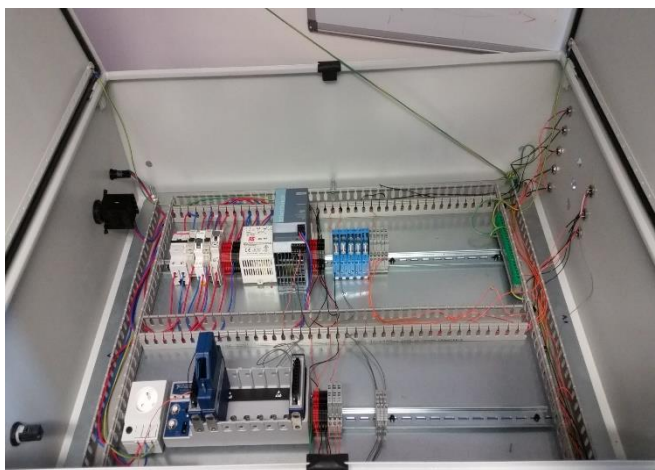


Fig 18: final result of the da ta acquisition box





Fig 19 : Pins connectors welding

4.2. Numerical validation

Goals:

The objective of this part can be divided into two : Firstly, to carry out a 3 D CFD study of the Moog 62 servovalve through the progressive variation of the spool displacement to determine its performance through the determination of the following parameters by imposing a variation total pressure between inlet and outlet equal to $\Delta p_{total} = 70$ bar:

- 1- detailed losses through the servovalve
- 2- determination of the flow rate corresponding to a $\Delta p_{total} = 70$ bar through the valve for different displacement of the spool
- 3- visualization of the speed and pressure field
- 4- determination of the angle of the jet at the orifices.

Second, build the full model of the linear actuated servovalve to determine:

- 1- the size of the linear actuator
- 2- the size of the return springs
- 3- determination of the flow rate and pressure drop by imposing $\Delta p_{total} = 70$ bar
- 4- Comparison of flow rates and pressure drop Ansysfluent VS Amesim

4.2.1 Computational fluid dynamic (CFD) with Ansysfluent

CFD tool is particularly suitable for the characterization of flow-pressure behaviour. It allows a consistent and precise description of three-dimensional phenomena and the coupling of different physical phenomena.

The evaluation of the constitutive law by the 3D CFD calculation is ruled, in order of importance, by:

1. the scope of the study (Extraction of the fluid volume, physical properties, boundary conditions);
2. the mesh type and size;
3. the boundary conditions;
4. the numerical scheme used;
5. the turbulence model used.
6. the result of the simulation;

Goals:

The goal here is to calculate using Ansysfluent the detailed pressure drops across the valve and the flow rate through the valve by imposing a $\Delta p_{total} = 70$ bar between the inlet and the outlet and varying the spool's displacement. This study is based on the progressive variation of the position of the spool in steps of 0.1mm over an interval of 0-1mm. This study also allows a detailed study of the singular pressure drops across the valve.

The CFD study of the servo valve performed aims to study the pressure losses through the servo valve and to compare them to the model produced on Amesim. It also allowed a study of the velocity field, the angle of the jet and the force of the fluid.

4.2.1.1 Description of geometry and volume extraction for the CFD simulation

Figure 20 below shows user ports A and B and ports P and T respectively connected to the pump (P) and reservoir(T). The volume in blue represents the fluid volume after extraction and the arrows the direction of flow of the fluid from port P to T through A then B.

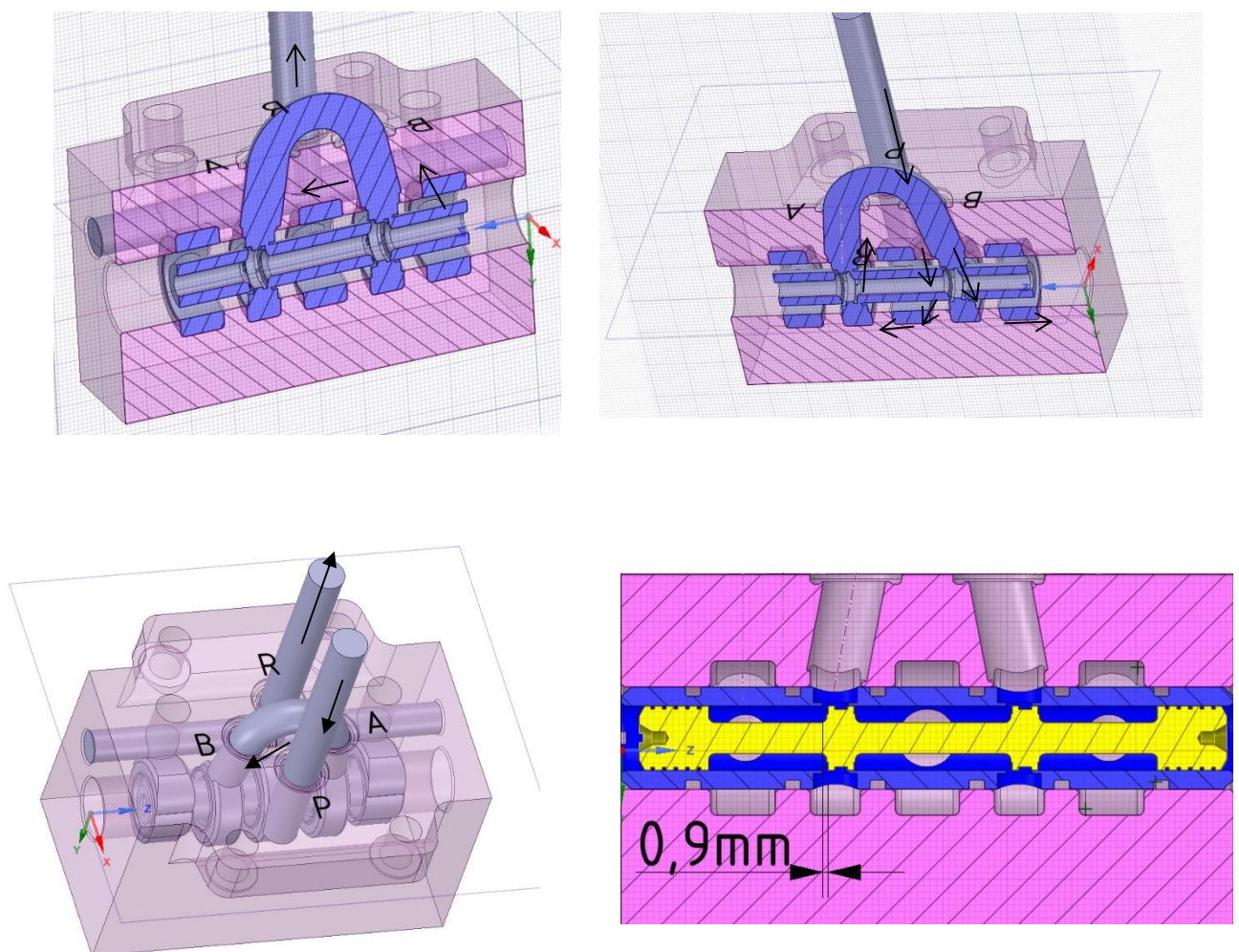


Fig 20: Path followed by the fluid

The servo valve consists of the assembly of the sleeve, the spool and the outer block.

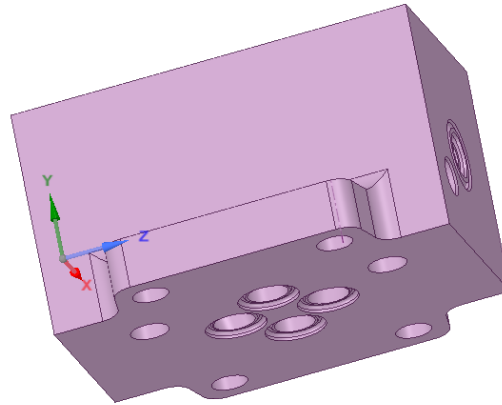


Figure 21: global view of the valve 3D model

4.2.1.2. Valve Assembly and volume extraction

Before the fluid volume extraction to be studied, the three components of the servo valve (spool, sleeve, external block) are assembled correctly and with a well-defined movement of the spool (mobile part) relative to the sleeve (fixed part).

Figures 23 and 24 show the assembly and extraction of the fluid volume, respectively.

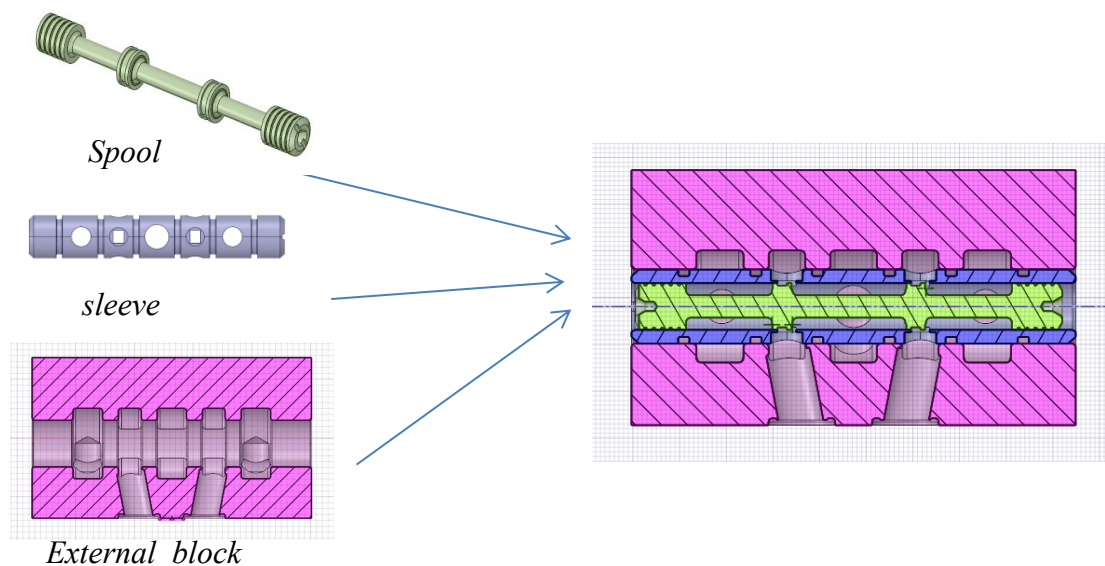


Fig 22: servo valve assembly

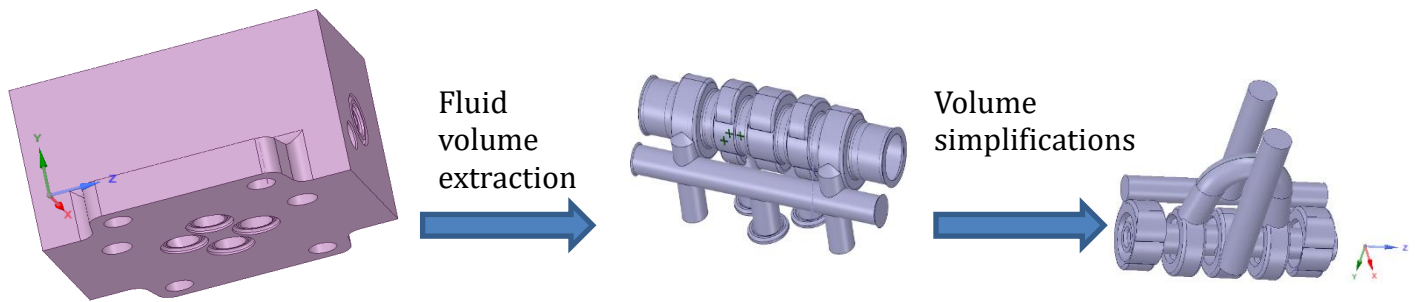


Fig 23: Fluid volume extraction and simplification

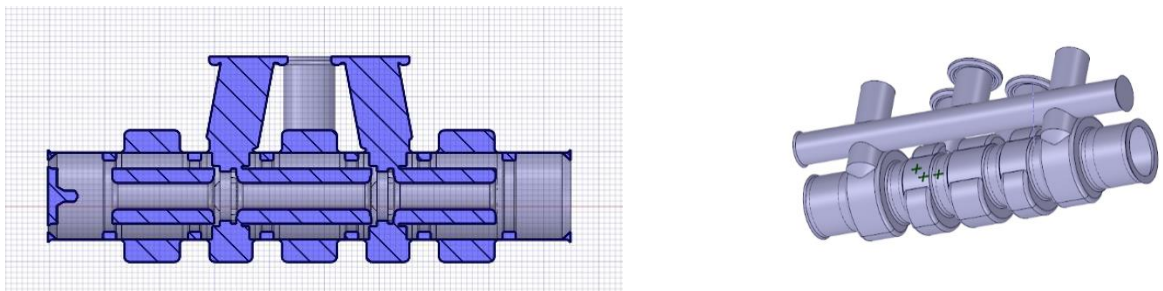
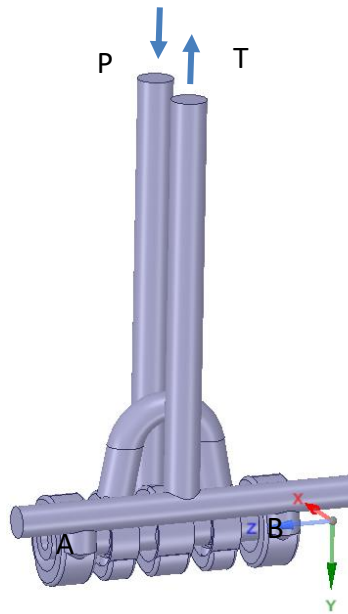


Fig 24: Transversal section of the fluid volume

4.2.1.3 Preparation and simplification of the fluid volume for the CFD

In general, in CFD it is important to simplify the fluid volume after extraction to make calculations easier. However, we must be reassured that these simplifications have a negligible influence on the final result. In the present case, the following simplifications have been made:

- Leakages between the spool and the sleeve are not taken into account
- Ports A and B are connected to reduce the number of boundary conditions (it is like connecting them with a user like an hydraulic cylinder)
- Extension of a distance $L = 10 \times \text{diameter}$ is added at ports P and T to move away from the boundary conditions of the system studied

*Figure 25: simplified*

4.2.1.4. 3D model in quasi-stationary approach

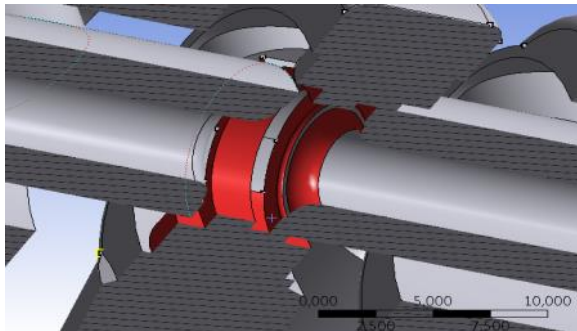
The quasi-stationary approach consists of carrying out a succession of simulations in which the only variable is the position of the spool relative to the fixed parts of the distributor. A set of ten operating points is carried out for this study.

4.2.1.5 Meshing

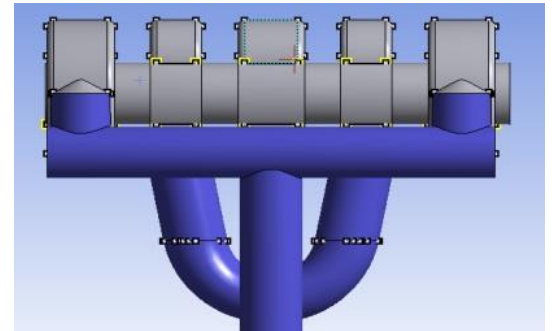
In front of the complexity of the geometry, a “**Cutcell**” mesh which is polyhedral and predominantly hexahedral was produced using **Ansys**-meshing.

Each area of the geometry has a specific refinement. Each area refinement allows to describe a complex flow subjected to strong speed gradient.

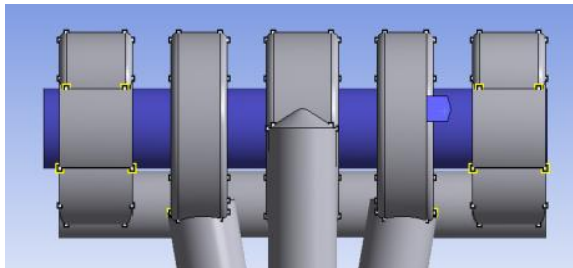
The smallest meshes are therefore located close to the walls and restrictions. We can distinguish four types of walls. **Figure 26** illustrates different areas in question.



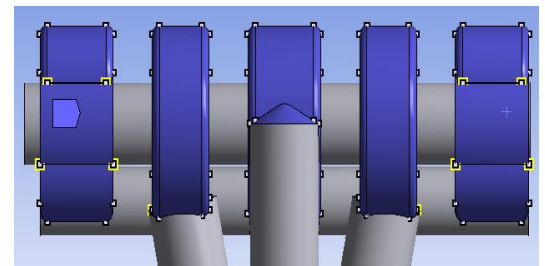
Area 1



Area 2



Area 3



Area 4

Fig 26 : Mesh sizes

Refined zone	Mesh size (mm)
Area1	0.075
Area 2	0.2
Area 3	0.3
Area 4	0.7

Tab 3: Mesh sizes for different areas

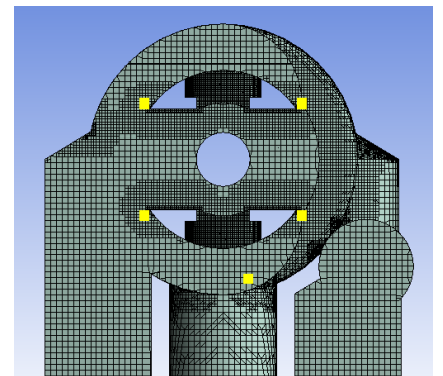
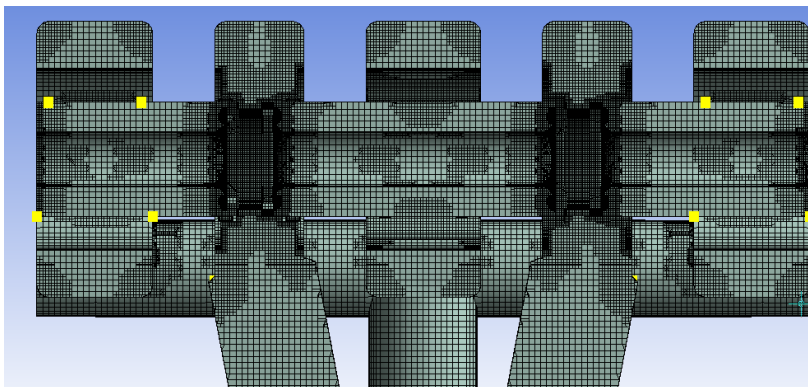


Figure 27: Mesh result for a 0.9 mm displacement

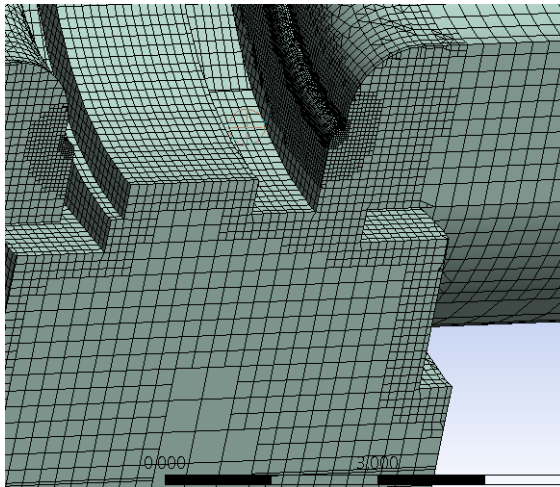


Fig 28-A : Very fine mesh for the restriction

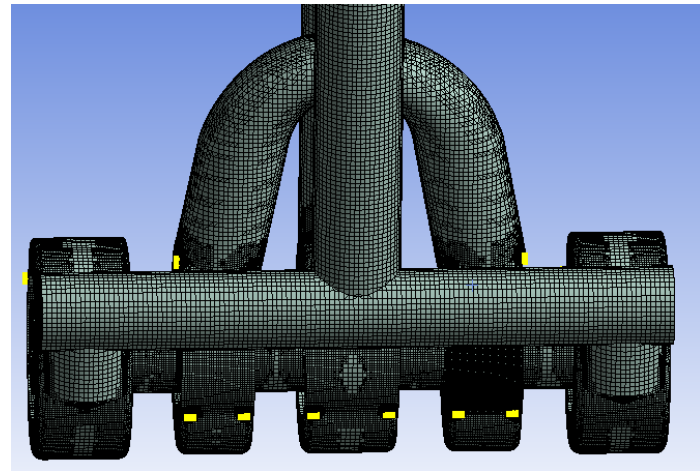


Fig 28-B: Global view of the meshing

4.2.1.6. Study of the sensitivity to the number of meshes for a 0.9 mm displacement

This meshes number sensitivity study is used to determine the total number of meshes for which the studied parameters become constant in order to limit the calculation times by using the minimum number of meshes necessary.

NB: this sensitivity study was carried out with a displacement of 0.9mm by imposing a flow rate equal to **57l / min** at the inlet and by observing the pressure at the inlet of port P and a pressure of 1 bar at the outlet of the valve.

Mesh number (millions)	Pressure at port p (bar)
0.88	57.7
1.2	58
1.4	59.1
1.9	59.3
2.24	59.3
3	59.28

Tab 4: Mesh number sensitivity study

It can be seen that the pressure results are stabilized more or less at 1.9 million meshes. So the various progressive variation simulations were carried out with a total number of meshes of about 2.5million.

4.2.1.7 Boundary conditions and properties of the fluid

The fluid used is an oil with a density of 870 kg / m³ and the dynamic viscosity is 0.0348 Pa-s.

The walls are considered hydraulically smooth. The study is carried out for different geometries based on a 0.1mm step progressive variation in position over a range of 0-1mm.

The boundary conditions are imposed with a static pressure imposed at inlet and outlet.

The study is conducted using the FLUENT software (developed by ANSYS) in an incompressible steady state (quasi-stationary approach).

All the simulations are carried out in a stationary and incompressible manner (no variation in fluid volume) for the quasi-stationary approach. The conditions imposed are an inlet pressure of the inlet = 70 bars and an outlet pressure of the outlet = 0 bar, thus making it possible to impose the total pressure drop equal to $\Delta p_{total} = 70$ bars.

➤ Fluid properties:

- Incompressible
- Density: 870 kg / m³
- Dynamic viscosity: 0.0348 Pa-s
- Temperature: 300k

➤ Boundary conditions:

- port P: a pressure $P_p = 70$ bar is imposed at the inlet
- port T: an outlet pressure of $P_T = 0$ bar is imposed

4.2.1.8. Numerical schemes

For the numerical resolution of the momentum and turbulence equations, we use mainly two schemes for reasons of their stability for the computation:

- **Turbulence equations:** 1st order "**First Order Upwind**". This is a simple and fast and stable scheme that produce a numerical result of satisfactory quality.
- **Equations of motion:** 2nd order "**Second Order Upwind**". This scheme allows a good compromise between stability, speed and precision of the calculations.

4.2.1.9. K-Epsilon model for turbulence

The turbulence model used is the k- ϵ Realizable model, "scalable wall function". It was selected for its "precision" / "calculation time" ratio which is better. compared to other turbulence models.

This turbulence model is one of the simplest and most recent that solves two separated transport equations for determining turbulent speed and length scale independently.

They are special due to a new formulation for the turbulent viscosity and a new transport equation for the dissipation rate ϵ . The term "Realizable" means that the model satisfies certain mathematical constraints on the Reynolds constraints and it is consistent with the physics of turbulent flows. An immediate benefit of this model is that it is more accurate in predicting the rate of diffusion in planar or circular jets. This new model is improved according to the standard model, in particular by improving the flow characteristics which include rotations or vortices.

4.2.1.10. Results of the CFD simulation

➤ Convergence results

The k-ε Realizable model was used and the convergence criterion of velocities, continuity, K and epsilon were defined at 10^{-6} . For a consistent result with Ansysfluent, it is good to have a convergence residual between 10^{-5} and 10^{-6} , which was respected in our case

(see **figure 29**)

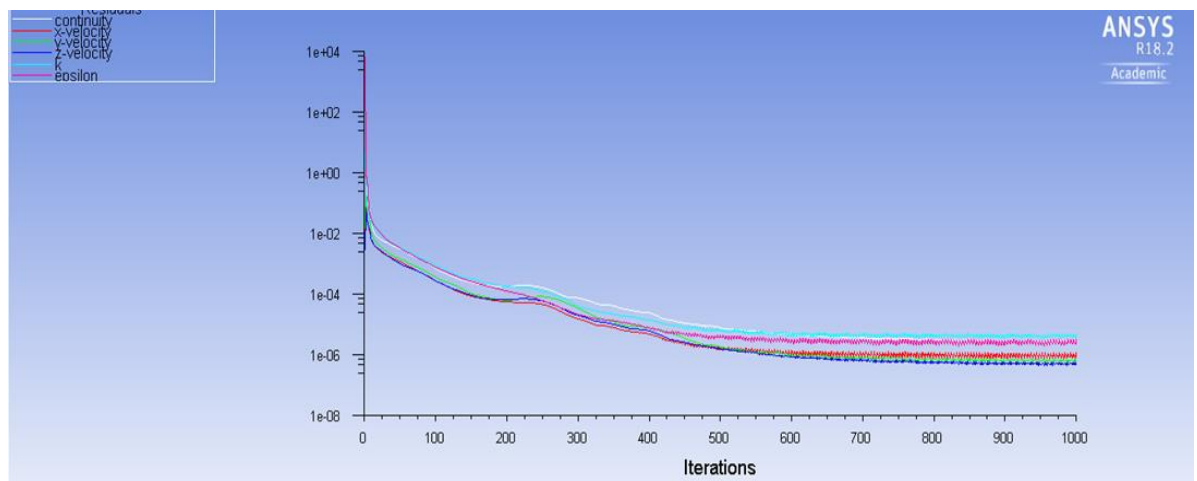
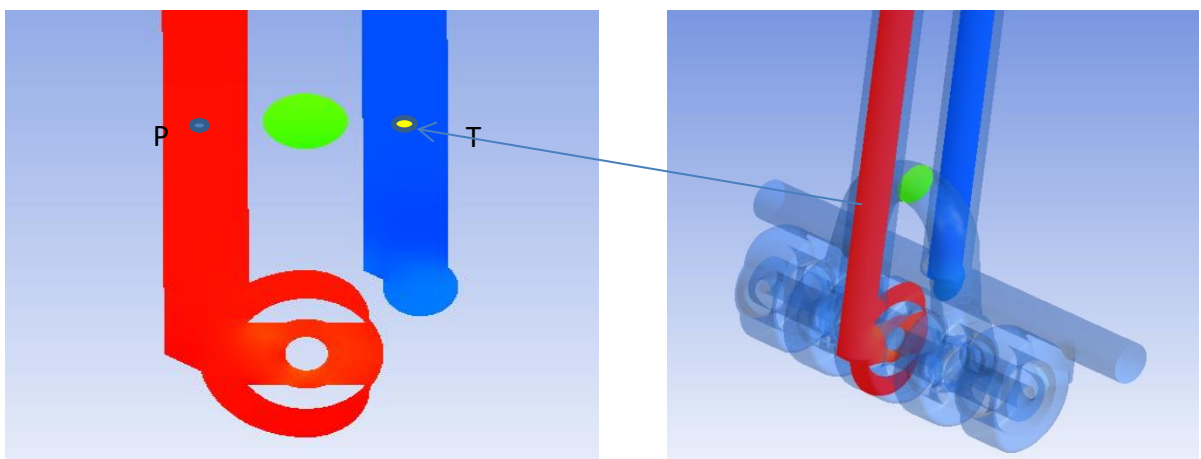


Figure 29 : convergence result

➤ Highlight of the points to study



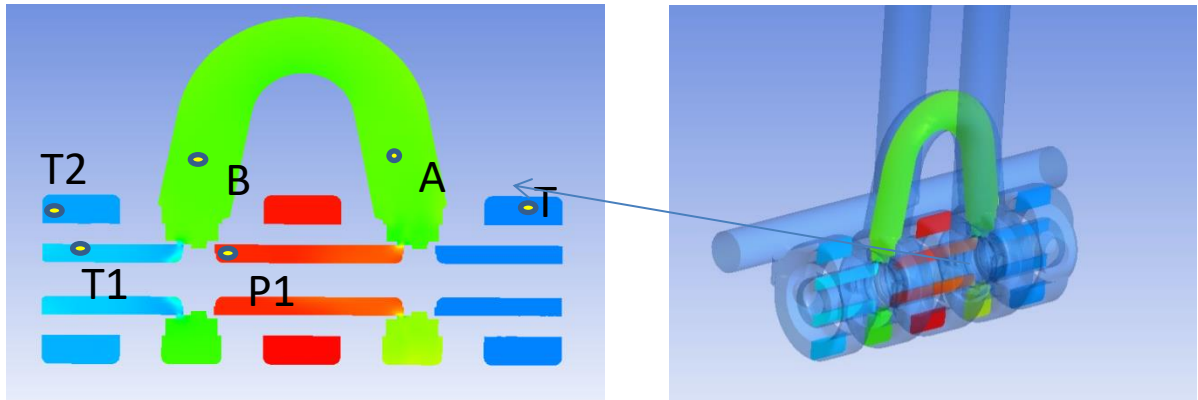


Fig 30 : points to study

The figures 30 above highlight the points to be studied subsequently. These points A, B, P and T are located in the same section. P1 is positioned just before fluid transition from P to A and T1 is just after the passage from B to T. T2 between T1 and T.

➤ Pressure field results

The areas in red represent the areas of high fluid pressure (valve inlet), in green the intermediate pressures and in blue the low pressures (reservoir).

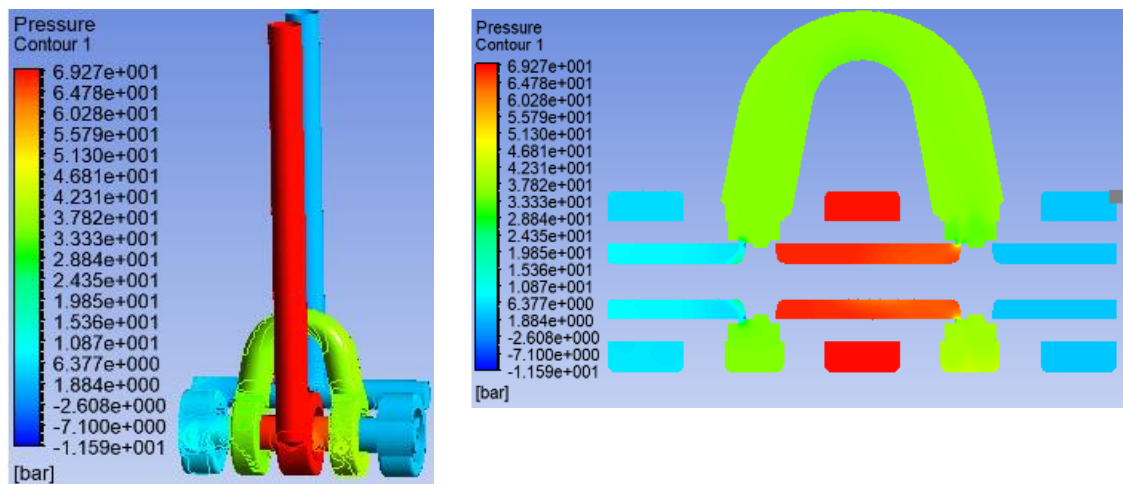


Fig 31-A : plan de coupe verticale au milieu des ports A et B

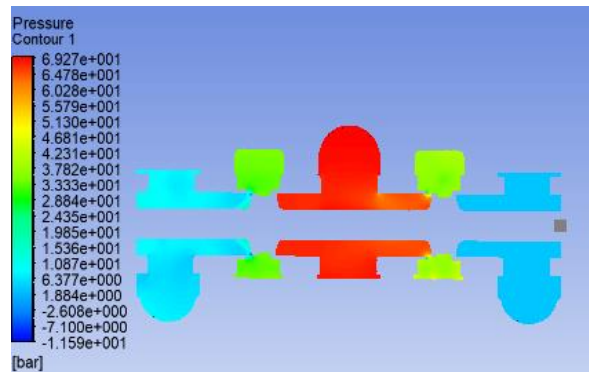


Fig 31-B : plan de coupe transversale au milieu des encoches

➤ Speed field for a 0.9mm displacement of the spool

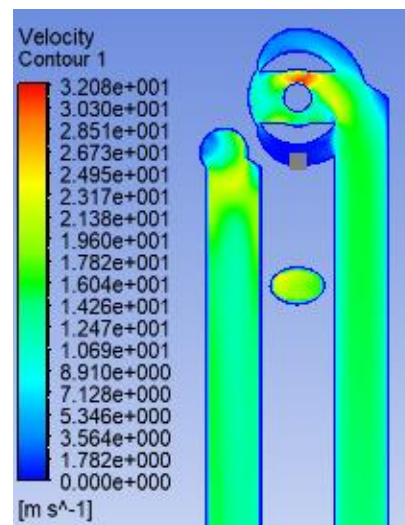


Fig 32-A: global Velocity field, section plane through port P and T

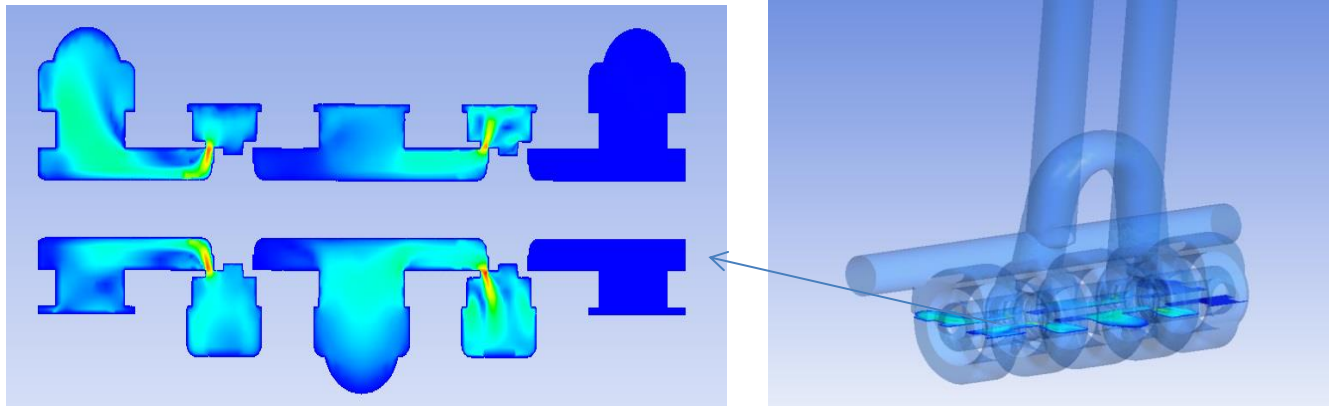


Fig 32-B: speed field section view through A and B

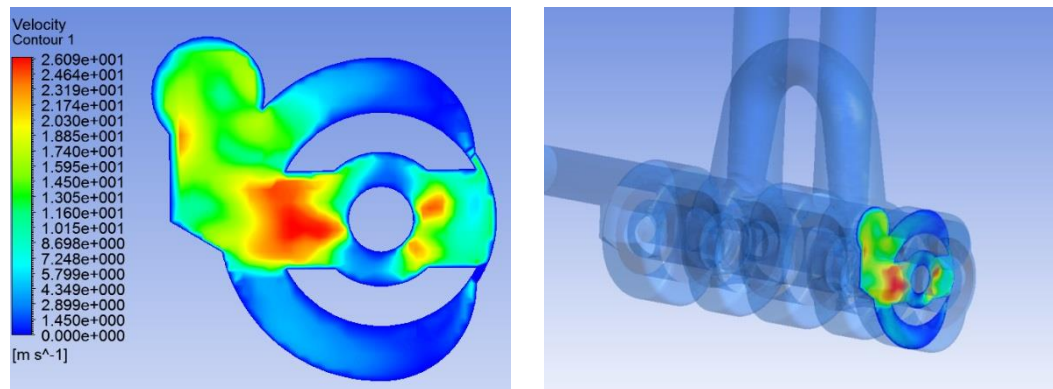


Fig 32-C: speed field fluid flow from B to T

- Jet's angle for a displacement of 0.9mm of the spool

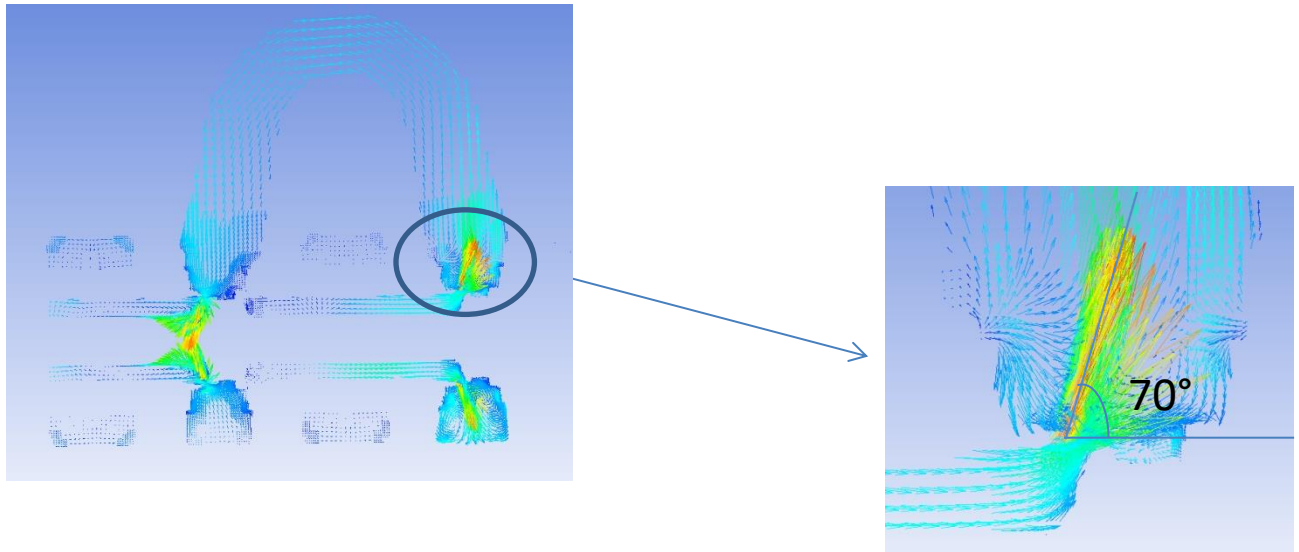


Fig 33: jet angle du jet for 0.9mm displacement

- Detailed result of pressure drop and flow obtained by imposing a $\Delta p = 70\text{bars}$ between input and output for a progressive displacement of 0.1 mm steps

The detailed calculation of the pressure drop through the valve is very important because it allows to locate the zones where the maximum losses occur and this will help in the future to make improvements in building the new valve.

	PRESSURE DROP (%)														
	displacement	P	P1	A	B	T1	T2	T	$\Delta p_{(p-p1)}$	$\Delta p_{(A-B)}$	$\Delta p_{(P1-A)}$	$\Delta p_{(B-T1)}$	$\Delta p_{(T1-T2)}$	$\Delta p_{(T2-T)}$	Total(%)
displacement	0,1mm	70	69,95	33,42	33,4	0,23	0,11	0	0,05	0,03	52,19	47,39	0,17	0,16	99,98
	0,2mm	70	69,8	35,3	35,2	0,69	0,36	0	0,2	0,14	49,29	49,30	0,47	0,51	99,91
	0,3mm	70	69,6	35,9	35,8	1,5	0,8	0	0,4	0,14	48,14	49,00	1,00	1,14	99,83
	0,4mm	70	69,3	36,4	36,3	2,4	1,5	0	0,7	0,14	47,00	48,43	1,29	2,14	99,70
	0,5mm	70	68,9	36	35,8	3,45	2,2	0	1,1	0,29	47,00	46,21	1,79	3,14	99,53
	0,6mm	70	68,3	35,9	35,8	5,14	3,23	0	1,7	0,14	46,29	43,80	2,73	4,61	99,27
	0,7mm	70	67,9	35,4	35,2	6,4	4	0	2,1	0,29	46,43	41,14	3,43	5,71	99,10
	0,8mm	70	67,25	35,6	35,23	8	5	0	2,75	0,53	45,21	38,90	4,29	7,14	98,82
	0,9mm	70	67,1	35,3	35,1	9,2	5,7	0	2,9	0,29	45,43	37,00	5,00	8,14	98,76
	1mm	70	66,4	35,8	35,7	10,8	6,9	0	3,6	0,14	43,71	35,57	5,57	9,86	98,46

Tab 5 : pressure drop in percentage

Note: for the percentage calculations above, the total pressure drop corresponding to 100% is 70bars.

	Pressure drop in bar(bar) and flow rate in litre/min																
	displacement	P	P1	A	B	T1	T2	T	$\Delta p_{(p-p1)}$	$\Delta p_{(p-A)}$	$\Delta p_{(B-T)}$	$\Delta p_{(A-B)}$	$\Delta p_{(P1-A)}$	$\Delta p_{(B-T1)}$	$\Delta p_{(T1-T2)}$	$\Delta p_{(T2-T)}$	Flow rate(l/min)
Displacement	0,1mm	70	69,95	33,4 2	33,4	0,23	0,11	0	0,05	36,58	33,4	0,02	36,53	33,17	0,12	0,11	8,14
	0,2mm	70	69,8	35,3	35,2	0,69	0,36	0	0,2	34,7	35,2	0,1	34,5	34,51	0,33	0,36	16,55
	0,3mm	70	69,6	35,9	35,8	1,5	0,8	0	0,4	34,1	35,8	0,1	33,7	34,3	0,7	0,8	24,55
	0,4mm	70	69,3	36,4	36,3	2,4	1,5	0	0,7	33,6	36,3	0,1	32,9	33,9	0,9	1,5	32,14
	0,5mm	70	68,9	36	35,8	3,45	2,2	0	1,1	34	35,8	0,2	32,9	32,35	1,25	2,2	37,93
	0,6mm	70	68,3	35,9	35,8	5,14	3,23	0	1,7	34,1	35,8	0,1	32,4	30,66	1,91	3,23	44,83
	0,7mm	70	67,9	35,4	35,2	6,4	4	0	2,1	34,6	35,2	0,2	32,5	28,8	2,4	4	51,24
	0,8mm	70	67,25	35,6	35,2	8	5	0	2,75	34,4	35,23	0,37	31,65	27,23	3	5	56,48
	0,9mm	70	67,1	35,3	35,1	9,2	5,7	0	2,9	34,7	35,1	0,2	31,8	25,9	3,5	5,7	60,00
	1mm	70	66,4	35,8	35,7	10,8	6,9	0	3,6	34,2	35,7	0,1	30,6	24,9	3,9	6,9	65,72

Tab 6: pressure drop in bar and flowrate L/MIN

Spool position (mm)	Imposed pressure drop (bar)	Flow rate obtained (l/min)
0.1	70	8.14
0.2	70	16.5
0.3	70	24.5
0.4	70	32.14
0.5	70	38
0.6	70	44.8

0.7	70	51.25
0.8	70	56.5
0.9	70	60
1	70	65.7

Tab 7: flow rate obtained for an imposed $\Delta P_{total}=70$ bar

4.2.2. Numerical modelling of the linear actuated servo valve and estimation of the force and size of the springs and the actuator with Amesim

Goals:

The main objective of this part is to model the complete valve (spool + linear actuator) using Amesim to determine:

- the size of the linear actuator
- The size of the return springs
- determination of the flow rate and pressure drop by imposing $\Delta p_{total} = 70$ bar
- Comparison of flow rates and pressure drop between Ansysfluent and Amesim

This servo valve is actuated by a voice-coil linear actuator which allows it to be controlled in position. Voice-coil actuation has a great advantage over motor torque in terms of energy consumption because the spring keeps the spool in a balanced position at rest, making the later not wasting energy at rest position.

An other advantage is that one stage is eliminated because it is directly actuated.

The design of the servo valve is done in several stages:

- Modeling of the spool and sleeve.
- Evaluation of the spring's stiffness by applying extreme conditions.
- Model of the actuator by interpreting the electromechanical equations of the linear actuator.
- Integration of the actuator into the hydraulic valve model.

As a reminder, this servo valve is single-stage and has an electrical part which is the actuator and a hydraulic part which are the spool and the sleeve. For this, the system was modelled in several stages:

4.2.2.1 Model of the hydraulic part without the linear actuator.

With Amesim, to model the sleeve and the spool, the geometric dimensions of these elements are taken from the CAD then inserted into Amesim.

With Amesim, it is possible to define the geometrical parameters of the sleeve and spool such as the section shapes and dimensions.

The properties of the oil are identical to those used in the simulation of the Ansysfluent model

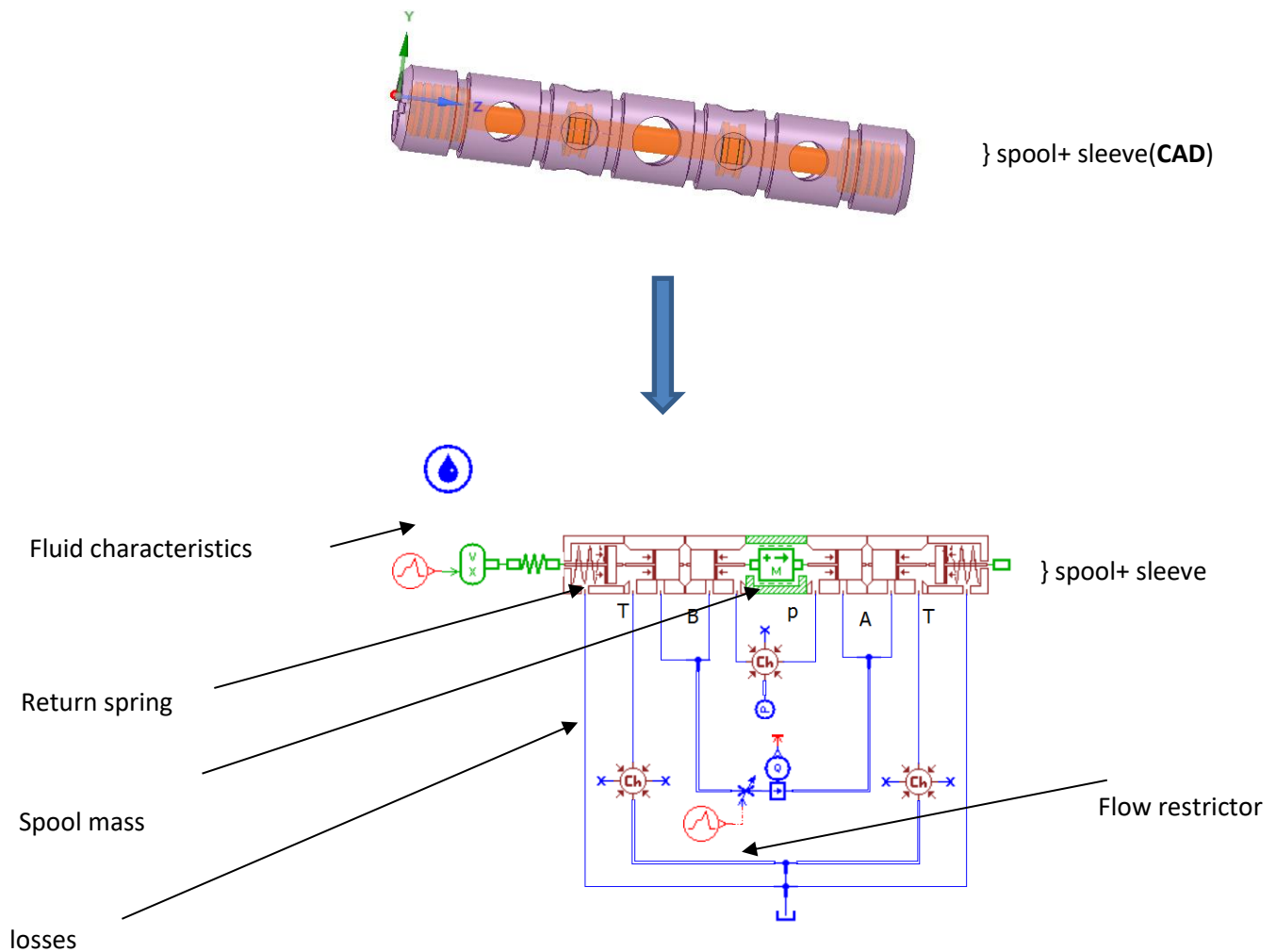


Figure 34 : simplified model without actuator

4.2.2.2. First estimation of the spring force for a maximum spool stroke (0.9mm).

The primary purpose is to evaluate the stiffness of the springs required to balance or return the spool to its rest position for a first estimation of the strength and size of the actuator. Unlike Ansysfluent, Amesim takes into account leakages and the friction forces between the spool and the sleeve.

➤ Parameters for Amesim simulation:

- Pressure port P: $P_p=210$ bar
- Pressure port T: $P_T=0$ bar
- Flow restrictor: $\Delta p=0.2$ bar
- displacement range of the spool: 0-0.9mm

These conditions are those the valve may be subjected to during its working cycle.

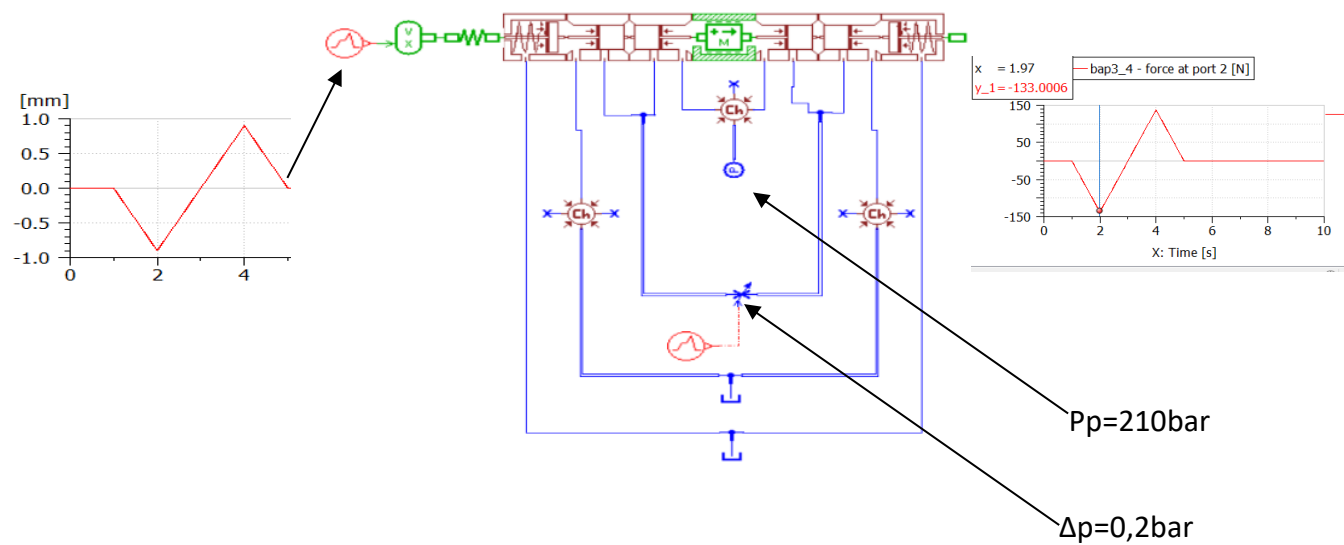


Figure 35 : Valve model in Amesim

Figure 35 Above shows the result of the required actuator's Force = 133 N in extreme operating conditions. Hence the choice of the following actuator:

Results:

- **Choice of the linear actuator with the vice coil technology:**
 - Maximum force the actuator can deliver, $F_{max}=150$ N
 - Diameter $D=60$ mm
 - Mass of the actuator's coil: $m=0,150$ kg
 - conversion coefficient: $K_w = 17$ N/vW

➤ **Choice of the spring:**

At the rest configuration, the spring's characteristics are the following:

- Force at rest position to maintain the spool at rest: **$F_0=150\text{ N}$**
- Stiffness constant: **$K=10\text{N/mm}$**
- initial length: **$L_0=10\text{mm}$**

4.2.2.3 Design of the valve integrating the actuator and regulating the PID controller

Creating the actuator model in Amesim requires interpreting the following electrical and electromechanical equations:

- $m \cdot \ddot{x} = -K_r \cdot x - C_v \cdot \dot{x} + F$
- $U - K_f \cdot \dot{x} = -R \cdot i + L \cdot \frac{di}{dt}$
- $F = K_f \cdot i$
- $E = K_v \cdot \frac{dx}{dt}$
- $K_v = K_f$

With **R**=coil resistance, **K_f**=force coefficient, **L**=impedance, **x**=displacement, **m**=actuator mass, **U**=voltage, **i**=current intensity, **K_r**=spring stiffness,

The actuator data are the following:

- Actuator mass **m**=0.15 kg
- Stiffness **k_r**=10N/mm
- Force coefficient **K_f**=48N/A
- damping coefficient **C_v**=10Ns/m
- coil resistance **R_b**= 8ohm
- Inductance **L**=0.008H

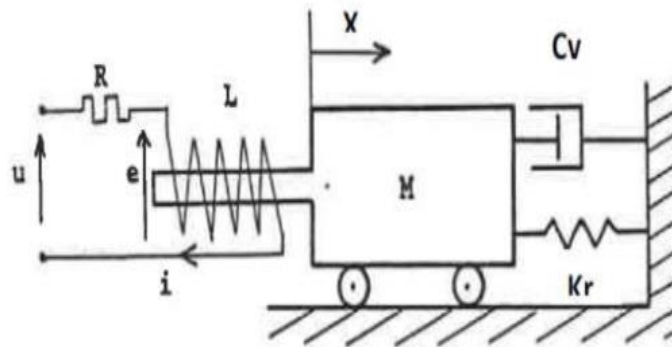


Figure 36: electromechanical scheme of the actuator

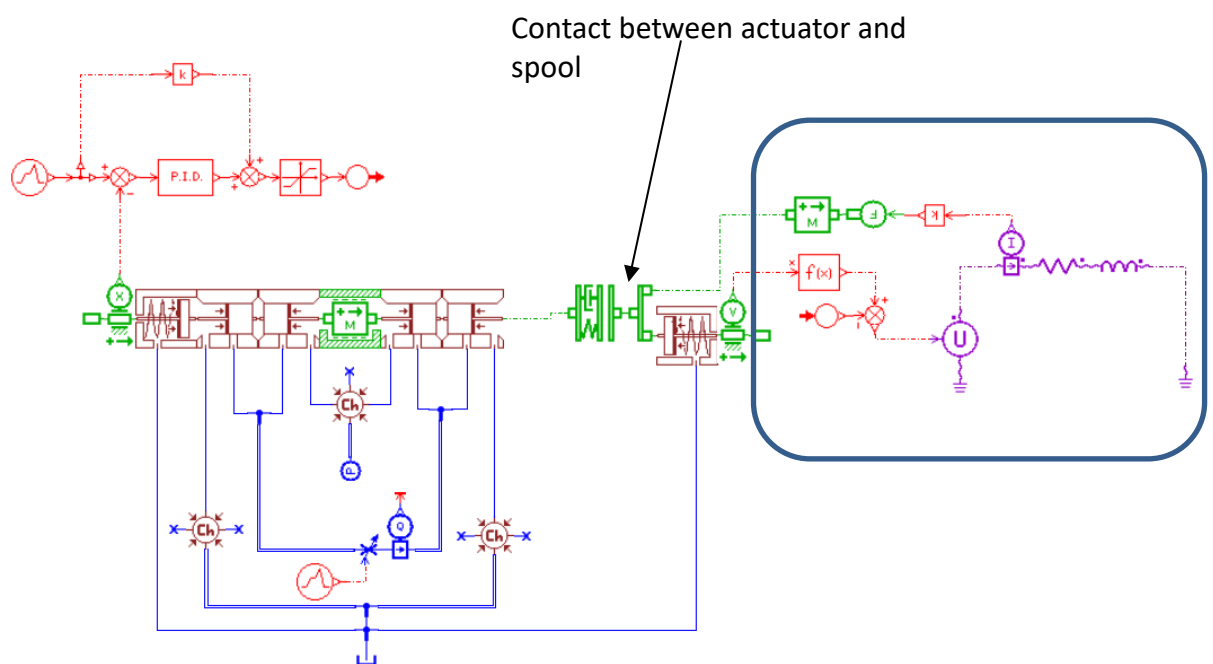
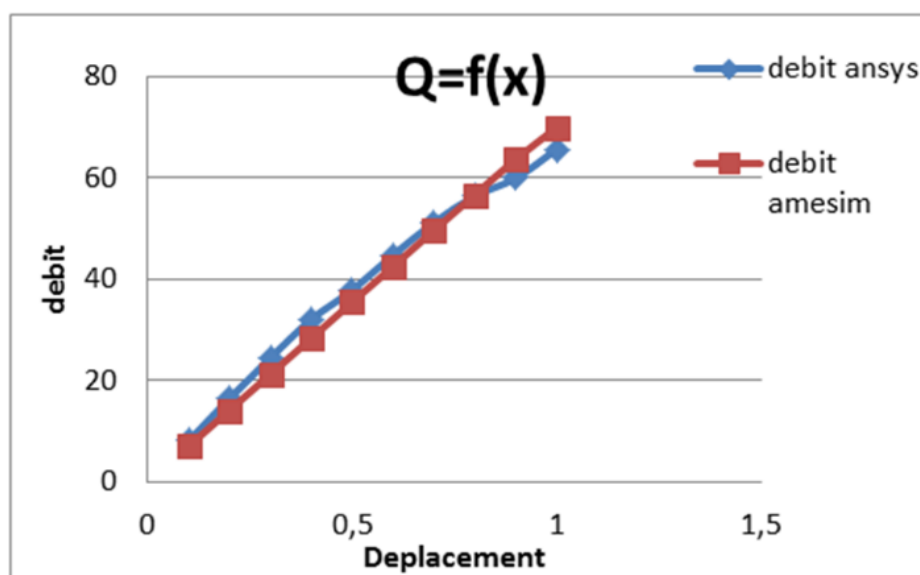


Figure 37: complete model valve + linear actuator

For the validation of the model, a comparison of the results of the flow rate and pressure drops obtained from Ansysfluent and Amesim simulation is necessary. Remember, however, that the two calculators use different methods of solving equations. In fact Ansys solves the equations with a 3D model while Amesim solves with a 2D one.

➤ **Flow rate results comparison Amesim VS Ansysfuent**

Diplacement (mm)	flow ansys(LPM)	flow amesim(LPM)	error(%)
0,1	8,13	7,12	12,5
0,2	16,55	14,23	14,0
0,3	24,55	21,3	13,2
0,4	32,13	28,42	11,6
0,5	37,93	35,53	6,3
0,6	44,82	42,6	5,0
0,7	51,24	49,7	3,0
0,8	56,48	56,73	-0,4
0,9	60	63,73	-6,2
1	65,72	70	-6,5

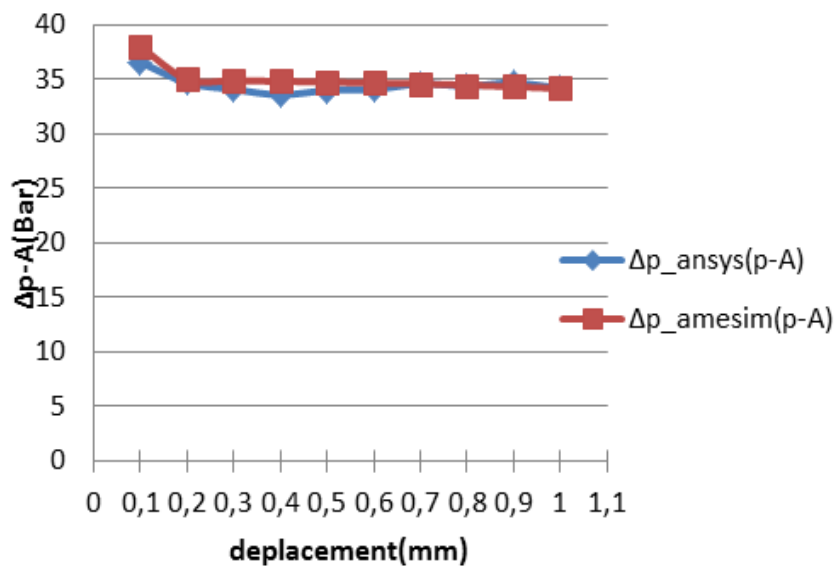


Tab 8: flow rate comparaison ANSYS VS AMESIM

From the flow rate comparison Ansys Vs Amesim (**table 8**), it appears that the relative error between the two softwares varies between **-6 and 13 %** which is relatively good. This difference is due to the fact that Ansys solves the problem in 3D while Amesim use a 2D model. In addition, some assumptions were made to simplify each model.

➤ **Comparison $\Delta p(p-A)$ Ansys-Amesim**

displacement(mm)	$\Delta p_{\text{ansys}}(p-A)(\text{bar})$	$\Delta p_{\text{amesim}}(p-A) (\text{bar})$	error(%)
0,1	36,58	38	3,74
0,2	34,7	35	0,86
0,3	34,1	34,9	2,29
0,4	33,6	34,84	3,56
0,5	34	34,77	2,21
0,6	34,1	34,67	1,64
0,7	34,6	34,62	0,06
0,8	34,4	34,5	0,29
0,9	34,7	34,34	-1,05
1	34,2	34,18	-0,06

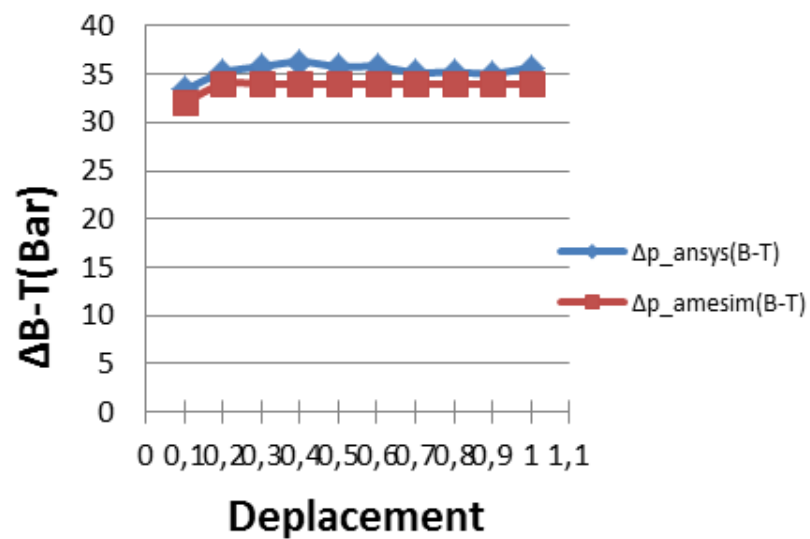


Tab 9: comparison $\Delta P(P-A)$ ANSYS AND AMESIM

For the $\Delta p(P-A)$ comparison results, the relative error percentage is between **-1 et 4**.

➤ **Comparison $\Delta p(B-T)$ Ansys-Amesim**

Displacement (mm)	$\Delta p_{\text{ansys}}(B-T)(\text{bar})$	$\Delta p_{\text{amesim}}(B-T)(\text{bar})$
0,1	33,4	32,1
0,2	35,2	34
0,3	35,8	34
0,4	36,3	34
0,5	35,8	34
0,6	35,8	34
0,7	35,2	34
0,8	35,23	34
0,9	35,1	34
1	35,7	34



Tab 10: comparison $\Delta P(B-T)$ ANSYS vs AMESIM

➤ Flow rate comparison catalogue VS Ansysfuent.

displacement (mm)	Pressure drop imposed (bar)	Flow rate obtained Ansys (l/min)
0.1	70	8.14
0.2	70	16.5
0.3	70	24.5
0.4	70	32.14
0.5	70	38
0.6	70	44.8
0.7	70	51.25
0.8	70	56.5
0.9	70	60
1	70	65.7

Nominal conditions from catalogue Moog62 :
 $\Delta P_{\text{nominal}} = 70 \text{ bars @ } 57 \text{ l/min}$
 error percentage flow rate = 0,87%

Tab 11 : comparison catalogue (nominal) flow rate VS ANSYS

A comparison between the nominal flow rate in the catalogue and that obtained with Ansysfuent (**tab 11**) gives us a relative error of 0.87 %, which is a good result for a CFD simulation.

4.2 Conclusion and Proposition of an improvement of the servo valve

Conclusion

The Flow rate obtained for a 0.8mm displacement of the spool and $\Delta p_{\text{total}} = 70 \text{ bar}$ is 56.5l / min. These results are quite similar to the nominal pressure drop and flow conditions indicated in the catalogue for the Moog 62 servo valve ($Q_{\text{nominal}} = 57 \text{ L /min}$ for $\Delta p_{\text{nominal}} = 70 \text{ bars}$). There is also a small difference between the results of Ansys and Amesim. This is because the two calculators use different approaches in solving the equations and the simplifications between Ansys and Amesim differ a bit.

Proposition of an improvement of the servo valve:

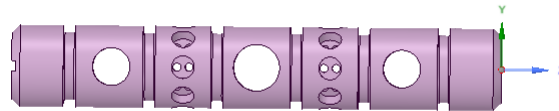
An improvement to reduce the size of the actuator can be made by replacing a rectangular hole on the sleeve with two cylindrical holes of equivalent total opening section.

The results of the Ansys simulation flow with this new geometry by imposing $\Delta p = 70\text{bars}$, which gives us about 57l / min. The jet angle approaches 90° (Figure 17), this considerably reduce the fluid reaction force on the spool and therefore, reduce the size of the actuator to be used.

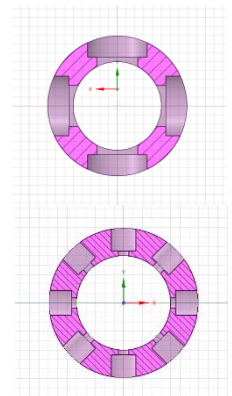
This situation can be compared to the displacement of 0.8 mm by imposing $\Delta p = 70\text{bars}$ (see table 6). In addition to that, it is easier to make cylindrical hole than rectangular one. The figures below highlight the difference between the two configurations:



Sleeve with rectangular holes



Sleeve with cylindrical holes



Transversal section view

Fig38: difference between the two orifice types

Notes: the total flow area with a completely open cylindrical orifice is substantially equal to that of the rectangular shape for a 0.8mm displacement.

-Results of the valve improvement:

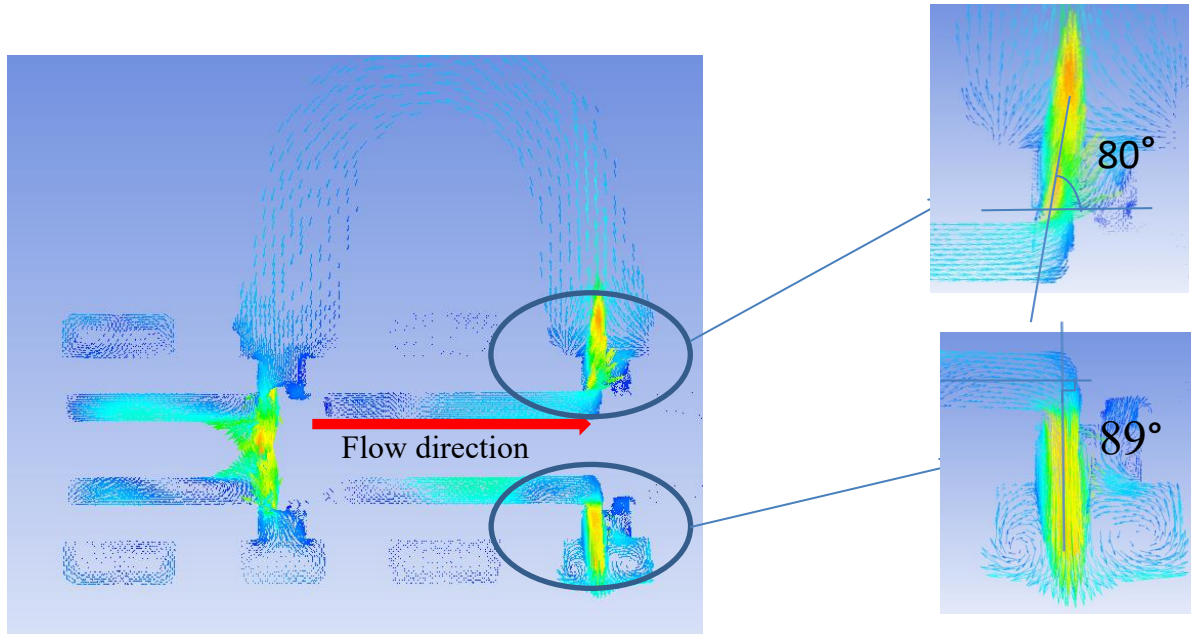


Fig39: Jet angle for the cylindrical hole configuration

Simulation conditions:

- Same as for the rectangular hole configuration
- identical total equivalent flow area for both configurations

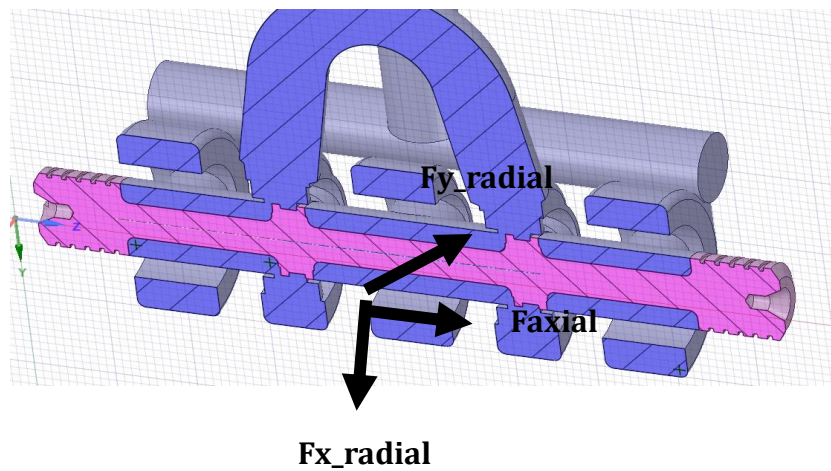


Fig 40: Fluid force on the sleeve

$$F_{axiale} = \rho Q \cos P$$

(formula 2)

Fluid force	Rectangular holes	Cylindrical holes
Faxial(N)	7,7	4,6
Fx_radial(N)	0,21	1,22
Fy radial(N)	0,29	1,22
Angle (°)	70	80 et 89
Flow rate (l/min)	56,5	55,7

Tab 12: comparison between the two configurations

The results of the two simulations give equal flow rates which confirms the equality of the fluid sections area of the two configurations.

We note that the jet angle increased from **70 °** to **80 °** and **89 °**. However, the force depends on the angle of the jet as indicated by “**formula 2**” above. The axial force decreased from **7.7** to **4.6N** which is a great benefit for the actuator whose size may be reduced.

5. WHAT I LEARNED DURING THE STAGE

5.1. Professional competencies acquired

These 6-months internship period was very enriching and allowed me to learn a lot of new things.



On a professional and organizational level, I had the opportunity to discover how the company operates and to better manage my working time according to deadlines that had to be met throughout the internship.

I also learned the study approach to design a fluid power component. Mainly This internship allowed me to discover a new discipline of fluid dynamics and CFD which I am passionate about now.

I also improved in self-employment and in finding information to solve a problem.

I was lucky enough to attend a hydraulic drone mock-up show with the UTC Hydraulic team, which improved my presentation skills.

What I liked the most was the diversity of everyday life and the variety of topics covered. In fact It combined fluid dynamics, fluid power some electronics and control of fluid power.

On the technical level, for the realization of the bench, I learned to use working instruments such as a drill to make holes on the metal box, use of the soldering iron to weld electric wires to the connector ports, the use of the saw, and other materials. In summary, I was able to develop a certain skill in manual work.

I also enjoyed the beauty of automatic control of fluid power systems, the power of CFD tools in for simulations. Finally, I improved my knowledges of electrical and electronics by learning how to choose electrical and electronic components for a data acquisition system.

5.2. Software used

During the internship, I had the chance to learn the use of new softwares:

-Ansysfluent

I started out learning this CFD tool (calculation of flow rate, pressure drops, jet angle). In fact, this tool is very suitable for studying the behaviour of fluid in 3D. I learned how to do a full CFD study and how to interpret the results.

- Amesim

Unlike Ansysfluent, Amesim is very important software for multi-physics studies as in the case of my study where I learned to model a servo valve (Actuator+Hydraulic part)

6. CONCLUSION

At the end of this project I would say I am satisfied enough of the multidisciplinary aspect. Indeed, I was able to deepen my knowledge in mechanical design, in particularly in the field of fluid power. This internship provided me some basic understanding of hydraulic system control, CFD simulation and how to select electrical and electronics components for a data acquisition system.

The project was about designing a test bench, a linear actuated servo valve. However, given the length of the project and some delay in delivering some components, the bench was not mounted, and the tests were not carried out on the real platform.

The following points have been achieved:

- Numerical study and design of the system (bench + servo valve).
- Quotation and ordering of the material necessary for the assembly of the bench.
- Design and assembly of the data acquisition control box.

The rest of the project will be done by another intern after the bench being assembled by a technician. This work will consist of:

- Realize the control laws for the bench using “**Labview** software”.
- Perform the measurements on the Moog 62 servo valve and compare them with those in the catalogue to be able to validate the bench.
- Perform the experimental measurements on the voice-coil servo valve to better compare its performance with Amesim model.

7. GLOSSARY

- **Moog 62** : Existing servo valve model(torque-motor actuated) used to design the linear actuator one
- **Amesim**: Multi physics simulation software.



- **Ansysfluent**: CFD simulation software using finite volume method.

- **keps** : k-ε turbulent model

- **Voice-coil**:

electrodynamic actuator consisting of a moving coil whose winding is crossed perpendicularly by a fixed magnetic flux. This fixed flux B comes from a magnetic circuit. When a current i passes through the turns L of the coil, in reaction with the magnetic flux according to Laplace's law $F = BLi$, generate a mechanical force as result. This force is proportional to the current and reversible depending on the polarity of the current in the direction of the axis. This electrodynamic actuator technology is used for applications requiring precise control, high dynamics and reversible piloting. The mechanical endurance is several 100 Million cycles.

8. SOURCES

- Website Pack'Aéro mécatronique :

<https://www.packaero.com/mecatronique-de-pointe>.

- Electro hydraulic servo valve :

http://www.unilim.fr/pages_perso/thierry.cortier/Hydraulique_cours/co/Hydraulique_-_De_la_mecanique_des_fluides_a_la_transmission_de_Puissance_183.html

<http://www.dietzautomation.com/download/User%20Manual%20-%20Valve%20Expert%2004%20-%20Francais.pdf>

- Ansysfluent website :

<https://www.ansys.com/it-it/products/fluids/ansys-fluent>

- CETIM** : <https://www.cetim.fr/mecatheque/Veille-technologique/Les-travaux-de-recherche-en-hydraulique-dans-le-monde>

9. ANNEXES

9.1 List of figures

Figure1: global view of the platform

Figure 2: PACK'AERO location sites

Figure 3: Hydraulic tree shaker machine

Figure 4: Working principle of the Moog 62 servo valve

Figure 5: Schematic representation of the servo valve

Figure 6-a Spool central position

Figure 6-b: Spool left position

Figure 6-C: Spool right position

Figure 7: servo valve with linear actuator

Figure 8-a: linear actuator voice coil

Figure 8-b: Force orientation according to the magnetic field

Figure 9: general overview system bench-servo valve

Figure 10-A: flow measurement from A to B

Figure 10-B: flow measurement from A to R

figure 10 C: flow measurement from B to R

Figure 10-D: leakages and pressure drop

Figure 12: configuration for dynamic tests

Figure 13: Manifold

Figure 14-A: Flow rate from A to B

Figure 14-B: flow rate from A to T

Figure 14-C: Flow rate from B to T

Figure 14-D: leakages and pressure drop

Figure 15: Signal distribution (sensors+cards)

Figure 16: Box drilling holes process

Figure 17: rails fixation, components mounting on the supports and cabling

Figure 18: final result of the box

Figure 19: Pins connectors

Figure 20: Path followed by the fluid

Figure 21: global view of the valve 3D model

Fig 22: servo valve assembly

Figure 23: Fluid volume extraction and simplification

Fig 24: Transversal section of the fluid volume

Figure 25: simplified

Figure 26: Mesh sizes

Figure 27: Mesh result for a 0.9 mm displacement

Figure 28-A: Very fine mesh for the restriction

Figure 28-B: Global view of the meshing

Figure 29: convergence result

Figure 30: points to study

Figure 31-B : plan de coupe transversale au milieu des encoches

Figure 32-A: global Velocity field, section plane through port P and T

Figure 32-B: speed field section view through A and B

Figure 32-C: speed field fluid flow from B to T

Fig 33: jet angle du jet for 0.9mm displacement

Figure 34: simplified model without actuator

Figure 35: solution pour l'actionneur

Figure 36: electromechanical scheme of the actuator

Figure 37: complete model valve +linear actuator

Fig38: difference between the two orifice types

Fig39: Jet angle for the cylindrical hole configuration

Fig 40: Fluid force on the sleeve

9.2 Tables list

Tab 1: Hydraulic components list

Tab 2: data acquisition system components list

Tab 3: Mesh sizes for different areas

Tab 4:Mesh number sensitivity study

Tab 5: pressure drop in percentage

Tab 6: pressure drop in bar and flowrate L/MIN

Tab 7: flow rate obtained for an imposed $\Delta P_{total}=70$ bar

Tab 8: flow rate comparison ANSYS VS AMESIM

Tab 9: comparison $\Delta P(P-A)$ ANSYS AND AMESIM

Tab 10: comparison $\Delta P(B-T)$ ANSYS vs AMESIM

Tab 11: comparison catalogue nominal flow rate VS ANSYS

Tab 12: comparison between the two configurations



9.3 Nomenclature

- ΔP : pressure drop
- **BC** : boundaries conditions
- **P inlet, Pp** : inlet pressure
- **P outlet, PT** : outlet pressure
- $\Delta_{p\text{total}} = P_p - P_T$